

# Multi-layer Cross-attention is Provably Optimal for Multi-modal In-context Learning

Nicholas Barnfield<sup>1</sup>, Subhabrata Sen<sup>1</sup>, and Pragya Sur<sup>1</sup>

<sup>1</sup>Department of Statistics, Harvard University

May 19, 2026

## Abstract

Recent progress has rapidly advanced our understanding of the mechanisms underlying in-context learning in modern attention-based neural networks. However, existing results focus exclusively on unimodal data; in contrast, the theoretical underpinnings of in-context learning for multi-modal data remain poorly understood. We introduce a mathematically tractable framework for studying multi-modal learning and explore when transformer-like architectures can recover Bayes-optimal performance in-context. To model multi-modal problems, we assume the observed data arises from a latent factor model. Our first result comprises a negative take on expressibility: we prove that single-layer, linear self-attention fails to recover the Bayes-optimal predictor uniformly over the task distribution. To address this limitation, we introduce a novel, linearized cross-attention mechanism, which we study in the regime where both the number of cross-attention layers and the context length are large. We show that this cross-attention mechanism is provably Bayes optimal when optimized using gradient flow. Our results underscore the benefits of depth for in-context learning and establish the provable utility of cross-attention for multi-modal distributions.

## 1 Introduction

Large language models exhibit striking “in-context learning” (ICL) behavior [Brown et al., 2020]: given a sequence of input-output pairs for a new task, the model can infer the rule (the function from input to output) without any update to the model weights. This phenomenon has motivated a growing body of theoretical work that tries to understand when and how ICL succeeds in linearized attention-based models [Zhang et al., 2024a, Lu et al., 2025, Zhang et al., 2025].

Prior work on ICL has focused on unimodal data; in contrast, modern foundation models routinely process multi-modal data, such as text, images, video [Li et al., 2024], multi-omic data [Cui et al., 2025], etc.

In this work, we formulate and study an ICL problem on multi-modal data. Our main contributions are as follows:

- We introduce a statistical model for ICL on multi-modal data (Section 3). The proposed data distribution is a latent factor model where the factors are dependent across the data modalities, thereby capturing cross-modal commonalities and differences.
- We show that a single-layer, linear self-attention (LSA) model fails to achieve Bayes-optimal performance in-context over this class of data distributions (Section 4).

- We propose a multi-layer model with cross-attention (CA) plus self-attention (SA) and skip connections to solve the ICL problem in this context (Section 5). Linearizing the attention mechanism, we show that, even with a restriction of the model parameters, gradient flow on the population loss converges to the Bayes-optimal ICL predictor (Section 6).
- We complement our theory with numerical experiments in controlled and benchmark settings (Section 7). Synthetic experiments verify the qualitative predictions from our analyses. Experiments on corrupted avMNIST provide evidence that the new mechanisms identified by our theory are useful for multi-modal learning in conventional deep-learning architectures.

To highlight the technical challenge in our setting, note that prior theoretical works on ICL in a regression setting assume that the covariates are sampled from a fixed distribution (usually Gaussian), independent of the learning task [Zhang et al., 2024a, 2025, Lu et al., 2025]. Indeed, [Zhang et al., 2024a, 2025] note that the invariance of the covariate distribution across prompts is crucial in establishing the success of single-layer LSA. In sharp contrast, our multi-modal model exhibits covariate-shift across prompts. In addition, the prediction rule in a prompt is naturally coupled with the covariate distribution in our setting.

These differences are significant, and provably rule out single-layer LSA in our setup (Theorem 4.1). To overcome this issue, we introduce a novel multi-layer model based on linear cross-attention (LCA) and LSA. We show that it achieves Bayes-optimal performance for multi-modal ICL (Theorems 6.2 and 6.3). Our analyses deviate substantially from prior work, and we require new ideas to analyze the loss landscape in multi-modal problems. Our multi-layer architecture differs from standard ones found in the empirical literature in critical ways: in particular, in how we employ the CA mechanism and additional skip connections. We describe the differences further in Section 5. Our work forms the first to provide theoretical guarantees on versions of attention-based models that achieve Bayes-optimal performance in multimodal ICL.

## 2 Prior work

ICL capabilities of large language models were first noted in [Brown et al., 2020]. These observations motivated significant recent research on the foundations of ICL. Early investigation focused on the expressivity of transformers [Bai et al., 2023, Akyürek et al., 2023, Garg et al., 2022], demonstrating that their ICL capabilities enable them to implement common statistical algorithms. Connections with meta-learning and variants of gradient descent were noted in [Von Oswald et al., 2023, Ahn et al., 2023, Zhang et al., 2024b]. Generalization and stability properties of ICL were studied in [Li et al., 2023], while a Bayesian interpretation was offered in [Xie et al., 2022].

Training dynamics of attention-based models and ICL performance of the trained models have also been investigated. Perhaps the closest to our work is [Zhang et al., 2024a], which studies ICL for regression, demonstrating that a single-layer LSA model trained by gradient flow on the population loss learns the Bayes-optimal predictor. Subsequently, gradient flow or descent dynamics for multi-head self-attention were studied in [Chen et al., 2024, Zhang et al., 2025]. The recent work [Huang et al., 2023] goes beyond linearized attention models, and studies gradient descent on stylized one-layer transformers with non-linear softmax attention.

More recently, ICL has been studied for a wider variety of models ranging from Gaussian mixture classification and clustering to non-parametric regression [Shen et al., 2025, Maulen-Soto et al., 2025, Ma et al., 2025, Ching et al., 2026]. Attention-based models have also been studied as Gaussian sequence multi-index models [Cui et al., 2024, Arnaboldi et al., 2025, Troiani et al., 2025] and on sparse-token classification tasks

[Oymak et al., 2023, Barnfield et al., 2025], although ICL was not a key focus in these works. ICL performance for infinite token dimension was studied in [Lu et al., 2025, Letey et al., 2025]; see also [Wu et al., 2024] for the impact of the number of pre-training tasks in case of finite token dimension. Despite this extensive literature, these prior works are restricted to data arising from a single mode, whereas we focus on ICL for multi-modal data.

In diverse artificial intelligence problems, multi-modal learning—combining information from varied modes, e.g., text, image, video—is known to improve prediction, reasoning and learning capabilities. Although examined extensively in empirical studies [Radford et al., 2021, Alayrac et al., 2022, Jaegle et al., 2021, Wang et al., 2024], this setting is far from understood from a rigorous standpoint. Bridging this theoretical gap is a primary aim of our manuscript. Specifically, multi-modal learning is useful when the modes share common information. To capture this, we use latent variable models that have been widely used in statistical estimation for studying multi-modal data [Nandy and Ma, 2024, Ding et al., 2022, Mergny and Zdeborová, 2025, Keup and Zdeborová, 2025, Deshpande et al., 2018, Yang et al., 2025, Sergazinov et al., 2025]. But, these papers do not study ICL or attention-based models. On the theoretical end, [Liu et al., 2025, Gui et al., 2025, Cai et al., 2024] study multi-modal contrastive learning, but do not focus on ICL, which is the main focus of our present work.

### 3 Problem setup

We study a multi-modal framework where each prompt (task) provides a context of input–output examples; the inputs contain features from two distinct modalities. To model a natural multi-modal setting, we assume the data is drawn from a latent variable model. Unlike prior work on ICL, we allow the distribution of covariates to differ across tasks.

Formally, we observe  $N$  prompts (tasks) with (training) context length  $L$ . For each prompt  $j \in [N]$ , we observe a sequence  $(\bar{\mathbf{z}}_i^{(j)}, \tilde{\mathbf{z}}_i^{(j)}, y_i^{(j)})_{i=1}^L$  where  $y_i^{(j)} \in \mathbb{R}$  is a response and  $\bar{\mathbf{z}}_i^{(j)} \in \mathbb{R}^{d_1}, \tilde{\mathbf{z}}_i^{(j)} \in \mathbb{R}^{d_2}$  are two modalities of covariates, e.g., the modalities could represent an image and associated text annotation, respectively. In each prompt, we additionally observe a tuple  $(\bar{\mathbf{z}}_q^{(j)}, \tilde{\mathbf{z}}_q^{(j)}, y_q^{(j)})$ . We input the prompt and covariate pair  $(\bar{\mathbf{z}}_q^{(j)}, \tilde{\mathbf{z}}_q^{(j)})$  into the model, and it outputs a prediction  $\hat{y}_q^{(j)}$  for  $y_q^{(j)}$ . While training, the model weights are tuned to minimize the error in predicting the  $y_q$  values on the training prompts. To assess the ICL performance of the fitted model, we consider a fresh prompt, and study the prediction error of the fitted model on the  $y_q$  associated with the test prompt.

We now turn to a statistical model for the data. The covariates and response are generated via

$$\bar{\mathbf{z}}_i^{(j)} = u_i^{(j)} \mathbf{v}^{(j)} + \boldsymbol{\xi}_i^{(j)}, \quad \tilde{\mathbf{z}}_i^{(j)} = u_i^{(j)} \mathbf{r}^{(j)} + \boldsymbol{\eta}_i^{(j)}, \quad y_i^{(j)} = \zeta^{(j)} u_i^{(j)}. \quad (3.1)$$

The latent variable  $u_i^{(j)} \stackrel{\text{i.i.d.}}{\sim} \mathcal{N}(0, 1)$  is shared across both modalities and the response. The prompt-specific regression coefficient, which relates  $u_i^{(j)}$  to  $y_i^{(j)}$ , is given by  $\zeta^{(j)} \in \mathbb{R}$ . We assume that across prompts,  $\zeta^{(j)}$  are sampled i.i.d. from a distribution with mean 0 and variance 1. On the other hand,  $\mathbf{v}^{(j)} \in \mathbb{R}^{d_1}$  and  $\mathbf{r}^{(j)} \in \mathbb{R}^{d_2}$  are modality-specific vectors sampled i.i.d. across prompts. We defer precise assumptions about their distributions (Assumption 6.1). Finally,  $\boldsymbol{\xi}_i^{(j)} \stackrel{\text{i.i.d.}}{\sim} \mathcal{N}_{d_1}(0, \mathbf{I})$  and  $\boldsymbol{\eta}_i^{(j)} \stackrel{\text{i.i.d.}}{\sim} \mathcal{N}_{d_2}(0, \mathbf{I})$  are i.i.d. noise variables, and all unique variables on the right-hand side of (3.1) are mutually independent. The setup in (3.1) formalizes a fundamental idea underlying multi-modal machine learning: each modality provides a different (noisy) view of a common latent feature  $u$  which drives the response  $y$ .

Focusing on a single task, omitting the prompt superscript, stacking the covariates, we denote  $\mathbf{x}_i :=$

$\begin{bmatrix} \bar{\mathbf{z}}_i & \tilde{\mathbf{z}}_i \end{bmatrix}^\top$  and let  $d = d_1 + d_2$ . Then, in each prompt, the covariates and response are jointly Gaussian:

$$\begin{bmatrix} \mathbf{x}_i \\ y_i \end{bmatrix} \stackrel{\text{i.i.d.}}{\sim} \mathcal{N}_{d+1}(0, \boldsymbol{\Sigma}) \quad \text{with} \quad \boldsymbol{\Sigma} = \begin{bmatrix} \mathbf{I} + \mathbf{m}\mathbf{m}^\top & \zeta\mathbf{m} \\ \zeta\mathbf{m}^\top & \zeta^2 \end{bmatrix} \quad \text{and} \quad \mathbf{m} := \begin{bmatrix} \mathbf{v} \\ \mathbf{r} \end{bmatrix}. \quad (3.2)$$

Note, the same construction extends directly to three or more modalities by stacking all views into a single vector  $\mathbf{x}_i$ . The joint Gaussianity of the covariates and response allows us to write

$$y_i = \langle \mathbf{w}, \mathbf{x}_i \rangle + \varepsilon_i \quad \text{where} \quad \mathbf{w} = \frac{\zeta}{1 + \|\mathbf{m}\|^2} \mathbf{m} \quad \text{and} \quad \varepsilon_i \stackrel{\text{i.i.d.}}{\sim} \mathcal{N}(0, \zeta^2 / (1 + \|\mathbf{m}\|^2)). \quad (3.3)$$

Our goal is to learn the task-specific Bayes-optimal predictor  $\langle \mathbf{w}, \mathbf{x} \rangle$ . The setup (3.3) is reminiscent of the regression setting considered in [Zhang et al., 2024a, Lu et al., 2025, Zhang et al., 2025], yet presents several differences that make the learning problem significantly more difficult. Upon setting

$$\boldsymbol{\Lambda} := \text{Cov}(\mathbf{x} \mid \mathbf{m}) = \mathbf{I} + \mathbf{m}\mathbf{m}^\top$$

as the covariance of the covariates  $\{\mathbf{x}_i\}_{i=1}^L \cup \{\mathbf{x}_q\}$  conditioned on  $\mathbf{m}$ , we note that the distribution of covariates varies across prompts, since  $\mathbf{m}$  is sampled anew for each task. Furthermore, the task vector  $\mathbf{w}$  and covariate distribution are coupled through  $\mathbf{m}$ . Similarly, the variance of the additive noise and the task vector are coupled through the task-specific parameter  $\zeta$ . These dependencies invalidate prior ICL theory in our setup. As we will see below, this leads to the failure of single-layer linearized attention models previously shown to be successful for ICL when the covariate distribution does not change across prompts [Zhang et al., 2024a, 2025].

## 4 ICL and failure of LSA

In this section, we introduce ICL formally and show that a single-layer LSA model fails at the ICL task. To this end, we represent a single prompt by its covariate matrix  $\mathbf{X} := [\mathbf{x}_1, \dots, \mathbf{x}_L] \in \mathbb{R}^{d \times L}$  and target vector  $\mathbf{y} := [y_1, \dots, y_L]^\top \in \mathbb{R}^L$ .

We define the (non-learned) joint embedding matrix

$$\mathbf{E}_\mathbf{X} := \begin{bmatrix} \mathbf{X} & \mathbf{x}_q \\ \mathbf{y}^\top & 0 \end{bmatrix} = \begin{bmatrix} \mathbf{x}_1 & \mathbf{x}_2 & \cdots & \mathbf{x}_L & \mathbf{x}_q \\ y_1 & y_2 & \cdots & y_L & 0 \end{bmatrix} \in \mathbb{R}^{(d+1) \times (L+1)}$$

A model maps  $\mathbf{E}_\mathbf{X}$  to a scalar prediction  $\hat{y}_q$  for  $y_q$ . So far, the context length  $L$  is a free variable. In the subsequent discussion, it will be helpful to assume that the context length  $L = L_{\text{tr}}$  for prompts in the training data and  $L = L_{\text{te}}$  at test time. Our model architecture is independent of the context length, and thus this distinction is mostly for mathematical convenience.

**Formal ICL criterion.** For a new prompt with test context length  $L = L_{\text{te}}$ , let  $\hat{y}_q^{(\text{te})}$  denote the model prediction. We say a model *in-context learns* if

$$\hat{y}_q^{(\text{te})} \longrightarrow y_q^{\text{Bayes},(\text{te})} := \mathbb{E}[y_q^{(\text{te})} \mid \mathbf{m}^{(\text{te})}, \zeta^{(\text{te})}, \mathbf{x}_q^{(\text{te})}] = \langle \mathbf{w}^{(\text{te})}, \mathbf{x}_q^{(\text{te})} \rangle \quad (4.1)$$

almost surely (a.s.) as  $L_{\text{te}} \rightarrow \infty$ , where the a.s. statement is with respect to the randomness of the new prompt. In words, ICL in our framework is synonymous with the model recovering the *Bayes-optimal predictor*  $\langle \mathbf{w}^{(\text{te})}, \mathbf{x}_q^{(\text{te})} \rangle$  a.s. in the asymptotic  $L_{\text{te}} \rightarrow \infty$  limit. The asymptotic context-length criterion (4.1) matches the mathematical interpretation of ICL in prior work [Zhang et al., 2024a], yet unlike in the linear regression setup [Garg et al., 2022, Zhang et al., 2024a, Lu et al., 2025], the task vector  $\mathbf{w}$ , covariate distribution, and error variances are all coupled via latent variables  $\mathbf{m}$ ,  $\zeta$ . These dependencies make both the learning problem—and its analysis—substantially more difficult.

**Single-layer LSA baseline.** As a starting point, we study a simple baseline model and show its inability to in-context learn in our setting. We consider a single LSA layer acting on  $\mathbf{E}_X$  as seen in [Von Oswald et al., 2023, Ahn et al., 2023, Zhang et al., 2024a, Lu et al., 2025]. We write

$$\hat{y}_q = (\text{LSA}(\mathbf{E}_X; \theta))_{d+1, L+1} \quad \text{where} \quad \text{LSA}(\mathbf{E}_X; \theta) = \mathbf{E}_X + \mathbf{W}^{PV} \mathbf{E}_X \cdot (\mathbf{E}_X^\top \mathbf{W}^{KQ} \mathbf{E}_X / L) \quad (4.2)$$

and  $\theta = \{\mathbf{W}^{PV}, \mathbf{W}^{KQ}\}$  are learnable weight matrices. This model is a linearized analogue of a transformer block

$$\text{SA}(\mathbf{E}_X; \theta) = \mathbf{E}_X + \mathbf{W}^P \mathbf{W}^V \mathbf{E}_X \cdot \text{softmax}\left(\left(\mathbf{W}^K \mathbf{E}_X\right)^\top \mathbf{W}^Q \mathbf{E}_X / L\right) \quad (4.3)$$

—where now  $\theta = \{\mathbf{W}^P, \mathbf{W}^V, \mathbf{W}^K, \mathbf{W}^Q\}$ —without the MLP layer and layer normalization, and with tied parameters  $\mathbf{W}^{KQ} = (\mathbf{W}^K)^\top \mathbf{W}^Q$  and  $\mathbf{W}^{PV} = \mathbf{W}^P \mathbf{W}^V$ . Collapsing the key and query, and the projection and value weight matrices into single matrices for the LSA model differs from a practical transformer implementation, but is mathematically identical with regard to expressibility.

In demonstrating the success of the LSA model in unimodal ICL tasks, prior work [Zhang et al., 2024a] relies on proving that the parameters  $\theta$  can emulate a global, inverse, covariance  $\mathbf{\Lambda}^{-1}$ . However, in the multi-modal setting, as the covariance  $\mathbf{\Lambda}$  is random, no fixed parameter  $\theta$  can perform this inversion role and hence the LSA model fails at the ICL task as shown in Theorem 4.1.

**Theorem 4.1** (Single-layer LSA fails at ICL). *In the setting of Section 3, and assuming  $\|\mathbf{m}\|$  and  $\zeta$  are atomless<sup>1</sup>, no single-layer LSA predictor  $\hat{y}_q = (\text{LSA}(\mathbf{E}_X; \theta))_{d+1, L_{te}+1}$  can in-context learn in the sense of (4.1). In particular, for fixed  $\theta = \{\mathbf{W}^{PV}, \mathbf{W}^{KQ}\}$ ,  $\mathbb{P}\left(\lim_{L_{te} \rightarrow \infty} \hat{y}_q^{(te)} = y_q^{\text{Bayes}, (te)}\right) = 0$ .*

The above negative result (see proof in Appendix B) motivates examining more complex and deeper architectures for multimodal problems. Zhang et al. [2024a] demonstrates, for a particular shifting-covariate distribution, that the LSA model with weights obtained via gradient flow fails to in-context learn. In contrast, Theorem 4.1 establishes a negative result in full generality, showing that no parameter configuration will yield success at the ICL task under the multi-modal setting.

## 5 A multi-layer CA model

Motivated by Theorem 4.1, we propose a model where the embedding matrix is now learned and obtained from a deep network of layers akin to CA. Consider the model

$$\hat{y}_q = \text{SA}(\mathbf{E}_F; \theta)_{d+1, L+1} \quad \text{where} \quad \mathbf{E}_F := \begin{bmatrix} \mathbf{F} & \mathbf{x}_q \\ \mathbf{y}^\top & 0 \end{bmatrix} \quad \text{and} \quad \mathbf{F} := \text{CA}_T(\mathbf{X}; \gamma). \quad (5.1)$$

The above model (5.1) is a composition of a self-attention layer applied to an embedding  $\mathbf{E}_F$  that is in turn obtained by applying multiple layers of CA between the covariates  $\mathbf{X}$  and an evolving distribution  $\{\mathbf{F}_t\}_{t \geq 0}$  defined below. The final SA layer is defined analogously to (4.3) with parameters  $\theta$  and where  $\mathbf{E}_F$  now replaces  $\mathbf{E}_X$ . To define the CA model  $\text{CA}_T(\mathbf{X}; \gamma)$ , consider the recurrence

$$\mathbf{F}_t = \mathbf{F}_{t-1} + \mathbf{S}_{t-1} + \mathbf{A}_{t-1}, \quad \text{for } t = 1, \dots, T. \quad \text{Define } \mathbf{F} := \mathbf{F}_T := \text{CA}_T(\mathbf{X}; \gamma). \quad (5.2)$$

Above,  $\mathbf{A}_{t-1}$  is the output of an attention head,

$$\begin{aligned} \mathbf{A}_{t-1} &= \text{A}(\mathbf{Q}_{t-1}, \mathbf{K}_{t-1}, \mathbf{V}_{t-1}) := \mathbf{V}_{t-1} \cdot \text{softmax}\left(\mathbf{K}_{t-1}^\top \mathbf{Q}_{t-1} / L\right), \\ \mathbf{V}_{t-1} &= \mathbf{W}_{t-1}^V \mathbf{X}, \quad \mathbf{K}_{t-1} = \mathbf{W}_{t-1}^K \mathbf{X}, \quad \mathbf{Q}_{t-1} = \mathbf{W}_{t-1}^Q \mathbf{F}_{t-1}. \end{aligned} \quad (5.3)$$

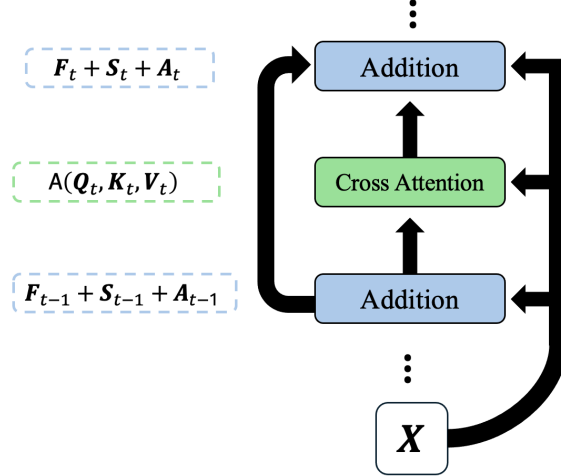


Figure 1: Re-injection of covariates  $\mathbf{X}$  throughout the  $\text{CA}_T$  ( $\text{LCA}_T$ ) embeddings. The propagation of the raw data  $\mathbf{X}$  occurs both through  $\mathbf{S}_t$  as well as through the CA block  $\mathbf{A}_t$ .

Here,  $\mathbf{W}_{t-1}^V, \mathbf{W}_{t-1}^K, \mathbf{W}_{t-1}^Q$  are learnable weight matrices, and  $\mathbf{S}_{t-1} = \mathbf{W}_{t-1}^S \mathbf{X}$  with learnable weight matrix  $\mathbf{W}_{t-1}^S$ . We take  $\mathbf{F}_0 = \mathbf{0}_{d \times L}$  to begin the recurrence and set  $\mathbf{F} = \mathbf{F}_T$  with  $T$  denoting the depth of the CA embedding. The weights of the embedding are  $\gamma = \{\mathbf{W}_t^V, \mathbf{W}_t^K, \mathbf{W}_t^Q, \mathbf{W}_t^S\}_{t=0}^{T-1}$ .

Notice that since the query matrix  $\mathbf{Q}_{t-1}$  depends on  $\mathbf{F}_{t-1}$ ,  $\mathbf{A}_{t-1}$  is an application of CA between the original data matrix  $\mathbf{X}$  and an evolving data distribution  $\mathbf{F}_{t-1}$ . For this reason, we view (5.1) as a  $T$ -layer CA model followed by a single layer of SA to obtain the final model output. The model includes the skip-connection of the previous layer input  $\mathbf{F}_{t-1}$  in each layer (5.2) resembling standard transformers. Diverging from conventional architectures [Vaswani et al., 2017], we also include a learnable skip-connection  $\mathbf{S}_{t-1}$  that injects the unaltered raw data  $\mathbf{X}$  into each layer as displayed in Figure 1. Taking inspiration from unrolled neural networks [Gregor and LeCun, 2010, Monga et al., 2021], the inclusion of  $\mathbf{S}_{t-1}$  was preceded by theoretical considerations—specifically, to yield embeddings  $\mathbf{E}_F$  with desirable properties—and later supported by ablation experiments (see Section 7 and Appendix G). As earlier, we use the bottom-right corner of the final output as our prediction  $\hat{y}_q$ .

Unlike conventional multimodal transformers, where cross-attention mediates interactions between different modalities [Tan and Bansal, 2019], our CA block repeatedly attends from the evolving state  $\mathbf{F}_t$  back to the fixed multimodal sequence  $\mathbf{X}$  itself. Together with the layer-wise re-injection term  $\mathbf{S}_t$ , this gives the model persistent access to the original input, heuristically enabling an iterative correction of the covariate representation; we examine the empirical relevance of these new architectural proposals through ablations in Section 7.

To ensure the analysis remains tractable, we replace the softmax with an identity map along the lines of Section 4 and prior theoretical literature on ICL [Von Oswald et al., 2023, Ahn et al., 2023, Zhang et al., 2024a, Lu et al., 2025]. This yields the linearization

$$\hat{y}_q = \text{LSA}(\mathbf{E}_F; \theta)_{d+1, L+1} \quad \text{where} \quad \mathbf{E}_F = \begin{bmatrix} \mathbf{F} & \mathbf{x}_q \\ \mathbf{y}^\top & 0 \end{bmatrix} \quad \mathbf{F} = \text{LCA}_T(\mathbf{X}; \gamma), \quad (5.4)$$

and  $\text{LCA}_T(\mathbf{X}; \gamma)$  denotes linearized CA where the softmax is replaced by the identity map in (5.3).

<sup>1</sup>For instance, any distribution on  $\mathbf{m}$  that is absolutely continuous with respect to the Lebesgue measure in  $\mathbb{R}^d$ .

For mathematical simplification, we do not include two key components of conventional transformers—layer normalization [Xiong et al., 2020] and non-linear activations (MLP layers). In Section 7 (Table 1), we incorporate these components, together with other refinements, into our architecture to empirically validate the mechanisms motivated by our theory. That said, note the model (5.4) is highly-nonlinear in  $\mathbf{X}$  and the final LSA readout is itself a non-linear (cubic) transformation of the learned embedding  $\mathbf{E}_F$ . Additionally, we notice qualitative similarities between the minima of the loss landscape both with and without layer normalization (Figure 4, Appendix F).

**Weight simplifications.** Thus far, the learnable weights have remained unconstrained. We now restrict their parameter space to ensure analytical tractability. To this end, we consider two simplifications. For both, we freeze  $\mathbf{W}_{t-1}^K = \mathbf{W}_{t-1}^Q = \mathbf{I}_d$ , and use an initialization strategy similar to [Zhang et al., 2024a] for  $\mathbf{W}^{PV}$  and  $\mathbf{W}^{KQ}$ ; see Appendix C.1.

**One-parameter model.** In the first case, we tie weights across layers and set  $\mathbf{W}_{t-1}^S = -\mathbf{W}_{t-1}^V = \alpha \mathbf{I}_d$  for all  $0 \leq t \leq T - 1$  where  $\alpha \in \mathbb{R}$  is a learnable scalar parameter. This gives a one-parameter model  $\hat{y}_q = f(\mathbf{X}, \mathbf{x}_q, \mathbf{y}; \alpha)$ .

**Two-parameter model.** For the second model, we instead set  $\mathbf{W}_{t-1}^S = \alpha \mathbf{I}_d$  and  $\mathbf{W}_{t-1}^V = \beta \mathbf{I}_d$  for all  $0 \leq t \leq T - 1$  where  $(\alpha, \beta) \in \mathbb{R}^2$  are learnable parameters, yielding a two-parameter model  $\hat{y}_q = f(\mathbf{X}, \mathbf{x}_q, \mathbf{y}; \alpha, \beta)$ .

The first model is recovered from the second by setting  $\beta = -\alpha$ . Since the one- and two-parameter models are subfamilies of the fully parameterized architecture (5.4), they help witness the expressibility of the unconstrained architecture. Importantly, these simplifications do not preclude optimality: we show in the following that the two restricted models already achieve Bayes-optimal prediction in the ICL setting when trained by gradient flow. Indeed, Figure 3 shows that less-restricted parametrizations exhibit qualitatively similar behavior as predicted in Section 6.

## 6 Training setup and main results

**Training setup.** Herein, we consider the one- and two-parameter models  $\hat{y}_q = f(\mathbf{X}, \mathbf{x}_q, \mathbf{y}; \theta)$  of Section 5 where  $\theta$  either denotes the parameters  $\alpha$  or  $(\alpha, \beta)$ . Starting with a set of  $N$  training prompts  $\{(\mathbf{x}_i^{(j)}, y_i^{(j)})_{i=1}^{L_{\text{tr}}} \cup (\mathbf{x}_q^{(j)}, y_q^{(j)})\}_{j=1}^N$ , given real-valued, continuous targets, it is natural to consider the empirical squared loss on the target query:  $\ell_{N, L_{\text{tr}}}(\theta) := \frac{1}{N} \sum_{j=1}^N (y_q^{(j)} - \hat{y}_q^{(j)})^2$ . As in prior work [Zhang et al., 2024a, Ahn et al., 2023], taking the number of training prompts  $N \rightarrow \infty$ , we operate on the population loss  $\ell_{L_{\text{tr}}}(\theta) := \lim_{N \rightarrow \infty} \ell_{N, L_{\text{tr}}}(\theta) = \mathbb{E}[(y_q - \hat{y}_q)^2]$ , where the expectation is taken with respect to the joint distribution detailed in Section 3. As a final reduction, we consider the asymptotic, training context-length regime and define the loss  $\ell(\theta) := \lim_{L_{\text{tr}} \rightarrow \infty} \ell_{L_{\text{tr}}}(\theta)$ . This regime is qualitatively similar to prior work [Zhang et al., 2024a] whereby one establishes the ICL capacity of the model at large context length, however our presentation diverges by taking the  $L_{\text{tr}} \rightarrow \infty$  limit before training on the loss function.

Having established the loss of interest, the training procedure for both variants of the CA model will simply be to run gradient flow on the limiting objective  $\ell$ . That is, the model parameters evolve according to the ordinary differential equation  $\frac{d}{dt} \theta_t = -\nabla \ell(\theta_t)$ , where  $(\theta_t)_{t \geq 0}$  is the trajectory of the parameters over the training horizon. Gradient flow can be seen as the limit of gradient descent in vanishing step size. Analyzing optimization in the gradient flow limit has enabled precise characterization of deep neural network training

dynamics [Saxe et al., 2013, Chizat and Bach, 2018]; this approach has been leveraged in previous studies on ICL as well [Zhang et al., 2024a, 2025].

**Main results.** We assume the following on the stacked modality-dependent vector  $\mathbf{m}$  from (3.2).

**Assumption 6.1** (Support of  $\|\mathbf{m}\|$ ). Assume  $\mathbf{m}$  has a continuous distribution and  $\underline{m} := \text{ess inf } \|\mathbf{m}\|^2 < \text{ess sup } \|\mathbf{m}\|^2 =: \bar{m} < \infty$  so that  $\|\mathbf{m}\|$  is a.s. bounded and non-degenerate.

The boundedness assumption on  $\mathbf{m}$  is mild, e.g., it holds as soon as the covariates are normalized, for instance  $\mathbf{x}_i \in [0, 1]^d$ . The density assumption is included for technical reasons. We do not believe it is intrinsically necessary for our results. We now present our main results. We show that a deep model of CA layers learns the Bayes-optimal prediction rule in-context for this multi-modal problem.

**Theorem 6.2** (One-parameter model optimality). *Assume the data generating process in Section 3 and Assumption 6.1. Run gradient flow on the loss  $\ell(\alpha)$  for the one-parameter model. Then, we have:*

1. *Gradient flow converges. Formally, letting  $(\alpha_{t,T})_{t \geq 0}$  denote the gradient flow trajectory for a CA stack of depth  $T$ , the limit  $\alpha_T^* := \lim_{t \rightarrow \infty} \alpha_{t,T}$  exists.*
2. *As  $T \rightarrow \infty$ ,  $\alpha_T^* \rightarrow \frac{2}{2+\bar{m}+\bar{m}} =: \alpha^*$  and the resulting predictor is Bayes optimal as the depth diverges. Formally,  $\lim_{T \rightarrow \infty} \lim_{L_{te} \rightarrow \infty} \hat{y}_q^{(te)} = y_q^{\text{Bayes,(te)}}$  a.s.*

We prove this result in Appendix D. Since prior linear-attention ICL analyses study fixed-depth, often single-layer, architectures, our infinite depth analysis necessitates a different strategy: we use novel convex-analytic, epi-convergence-style arguments to show that the one-parameter loss converges to a limiting objective whose minimizer can be analyzed. We now turn to the two-parameter setting.

**Theorem 6.3** (Two-parameter model optimality). *Assume the data generating process in Section 3, Assumption 6.1, and the regularity condition of Remark E.4. Run gradient flow on the loss  $\ell(\alpha, \beta)$  for the two-parameter model with initialization  $\beta_0 \in (-2/(\bar{m} + 1), 0)$  and  $\alpha_0 = \alpha^*(\beta_0)$  where  $\beta \mapsto \alpha^*(\beta)$  is defined in Appendix E.1. Then, we have the following:*

1. *Gradient flow converges. Formally, letting  $(\alpha_{t,T}, \beta_{t,T})_{t \geq 0}$  denote the gradient flow trajectory for a CA stack of depth  $T$ , the limit  $(\alpha_T^*, \beta_T^*) := \lim_{t \rightarrow \infty} (\alpha_{t,T}, \beta_{t,T})$  exists.*
2. *Suppose  $\lim_{T \rightarrow \infty} \beta_T^* \notin \{-2/(\bar{m} + 1), 0\}$ . Then, with  $\alpha^*$  as defined in Theorem 6.2, as  $T \rightarrow \infty$ ,  $\alpha_T^* \rightarrow \alpha^*$  and  $\beta_T^* \rightarrow -\alpha^*$ , and the resulting predictor is Bayes optimal as the depth grows. Formally,  $\lim_{T \rightarrow \infty} \lim_{L_{te} \rightarrow \infty} \hat{y}_q^{(te)} = y_q^{\text{Bayes,(te)}}$  a.s.*

The proof can be found in Appendix E. This theorem is considerably more involved and requires new proof techniques: since the loss is non-convex and non-coercive, the fixed-depth, gradient-flow limit  $(\alpha_T^*, \beta_T^*)$  can only be identified as a stationary point rather than a global minimizer. We handle this by reducing the problem to the evolution of  $\beta_T^*$  and showing, via a uniform derivative control, that, as  $T \rightarrow \infty$ , admissible stationary points collapse to the same limit. Theorem 6.3 shows that the limiting behavior of the two-parameter model mimics that of the one-parameter setting, whereby in both cases

gradient flow achieves the Bayes-optimal predictor.

A careful reading of the proof of Theorem 6.2 informs the choice of initialization in Theorem 6.3. Solving the recurrence (5.2) in the one-parameter model reveals  $\lim_{L_{te} \rightarrow \infty} \hat{y}_q^{te} = y_q^{\text{Bayes,(te)}} + e(\alpha)$  with error  $e(\alpha) = O(\|\mathbf{I} - \alpha \mathbf{\Lambda}\|^T)$ . A short calculation shows that  $e(\alpha) \rightarrow 0$  as  $T \rightarrow \infty$  when  $\alpha \in (0, 2/(\bar{m} + 1))$ . Given the correspondence between the two models, this lends to  $\beta_0 \in (-2/(\bar{m} + 1), 0)$  as a suitable initialization in the two-parameter setup. Moreover, the two-parameter loss  $\ell(\alpha, \beta)$  turns out to be quadratic in  $\alpha$  with explicit minimizer  $\alpha^*(\beta)$ , and hence starting at  $\alpha_0 = \alpha^*(\beta_0)$  becomes an obvious choice. This intuition is supported in a visualization of the loss landscape provided in Figure 4, Appendix F.

**The limiting parameter.** From the above discussion, the limiting parameter  $\alpha^* = 2/(2 + \underline{m} + \overline{m})$  suffices for Bayes optimality since  $e(\alpha) \rightarrow 0$  as  $T \rightarrow \infty$  when  $\alpha \in (0, 2/(\overline{m} + 1))$ . Recalling  $\mathbf{\Lambda} = \mathbf{I} + \mathbf{m}\mathbf{m}^\top$ , along the spike direction, the absolute value of the largest attainable eigenvalue is

$$\phi(\alpha) := \max\{|1 - \alpha(1 + \underline{m})|, |1 - \alpha(1 + \overline{m})|\}$$

and we note  $\alpha^* = \operatorname{argmin}_{\alpha \in \mathbb{R}} \phi(\alpha)$ . Interestingly, the limiting parameter  $\alpha^*$  coincides with the parametrization minimizing the worst-case error rate given by the spike contribution to  $e(\alpha)$ . Hence, Theorems 6.2 and 6.3 show that our CA models are minimax optimal in the large  $T$  and  $L_{\text{te}}$  limits.

**The role of depth.** Recall the embedding  $\mathbf{F} = \text{LCA}_T(\mathbf{X}; \gamma)$  (5.1) produced by the  $T$ -layer CA stack. Under mild conditions (and ignoring lower-order terms that vanish as  $L_{\text{te}} \rightarrow \infty$ ), the final prediction produced by the LSA readout has the schematic form  $\hat{y}_q^{(\text{te})} \approx \mathbf{w}^{(\text{te})\top} (\frac{1}{L_{\text{te}}} \mathbf{X}^{(\text{te})} \mathbf{F}^\top) \mathbf{x}_q^{(\text{te})}$  as shown in Appendix C (Lemma C.1). Thus, if the CA stack can enforce

$$\frac{1}{L_{\text{te}}} \mathbf{X}^{(\text{te})} \mathbf{F}^\top \rightarrow \mathbf{I}_d \quad \text{as } T \rightarrow \infty, \tag{6.1}$$

then  $\hat{y}_q^{(\text{te})} \rightarrow y_q^{\text{Bayes},(\text{te})}$  as both  $T \rightarrow \infty$  and  $L_{\text{te}} \rightarrow \infty$ . An instance where (6.1) can occur is if  $\mathbf{F} \approx \mathbf{\Lambda}^{-1} \mathbf{X}$ —that is, when  $\mathbf{F}$  whitens the covariates. Crucially, since the embedding  $\mathbf{F}$  is prompt-dependent, (6.1) is achievable despite  $\mathbf{\Lambda}$  being random: the model is not constrained to learn a single global inverse covariance, rather it can compute  $\mathbf{\Lambda}^{-1}$  implicitly from the prompt itself. Here lies the significance of the CA embedding as a denoising mechanism for the covariates, where, in contrast, a single LSA layer can only learn an average covariance, and thus fails to be Bayes-optimal.

## 7 Numerical experiments

We present three sets of experiments. First, on synthetic data generated under the assumptions of Section 3 and Assumption 6.1 (see Appendix H) we verify the qualitative predictions from Theorems 4.1, 6.2, and 6.3. Second, we train less-restricted parametrizations of the CA model (5.1), (5.2), and compare their behavior against the predictions of Section 6. Third, on a multi-modal benchmark dataset, we show that our theory-motivated architectural principles remain effective after replacing the linearized model (5.4) with standard deep-learning components—e.g. layer-normalization, MLP layers, and softmax attention. Furthermore, using ablations, we demonstrate the impact of our novel architectural components in (5.2), that is, CA between  $\mathbf{F}_t$  and  $\mathbf{X}$ , and reinjection of  $\mathbf{X}$  (through  $\mathbf{S}_t$ ).

**Validation of theoretical predictions.** In Figure 2 (Left), we observe the failure of the single-layer LSA model proved in Theorem 4.1. In contrast, LCA-based models achieve error rates which are several orders of magnitude smaller as  $L_{\text{te}}$  grows. Figure 2 (Right) shows the effect of depth in the  $\text{LCA}_T$  embedding, (5.4), in aiding model performance on the multi-modal ICL task. Despite the asymptotic frameworks in Theorems 6.2 and 6.3, we observe exceptional performance at moderate depth as anticipated by the geometric-rate error decay  $e(\alpha)$  discussed at the end of Section 6.

**Less-restricted parametrizations.** Our analysis restricts the LCA parametrization to simple one/two-parameter models with weight tying (recall definitions in the discussion preceding Section 6). Here, we train three less-restricted LCA parametrizations for  $(\mathbf{W}_t^S, \mathbf{W}_t^V)_{t=0}^{T-1}$  to investigate whether the predictions of Section 6 persist beyond tied scalar-identity weights (details in Appendix H). Specifically in Figure 3,

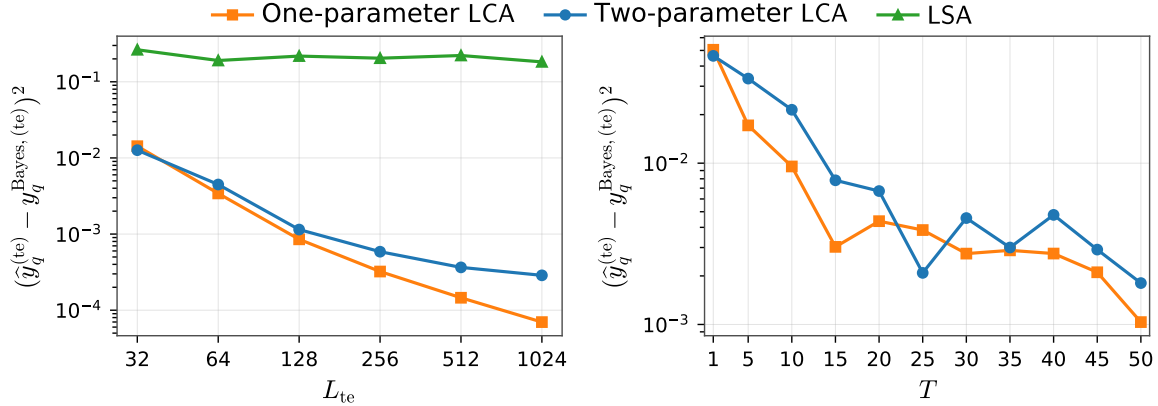


Figure 2: Prediction error for the one- and two-parameter LCA-based models and the LSA model. Left: ICL error at fixed depth for varying  $L_{te}$ . Right: ICL error at fixed  $L_{te}$  for varying depth  $T$ .

‘untied scalar’, ‘diagonal’, and ‘full-matrix’ respectively refer to  $(\mathbf{W}_t^S, \mathbf{W}_t^V) = (\alpha_t \mathbf{I}, \beta_t \mathbf{I})$  with  $(\alpha_t, \beta_t)_{t=0}^{T-1}$  learnable,  $(\mathbf{W}_t^S, \mathbf{W}_t^V) = (\text{diag}(\mathbf{b}_t), \text{diag}(\mathbf{b}_t))$  with vectors  $(\mathbf{b}_t, \mathbf{b}_t)_{t=0}^{T-1}$  learnable, and  $(\mathbf{W}_t^S, \mathbf{W}_t^V)$  taken as full matrices with all entries learnable. Figure 3 (Left) displays the normalized traces  $\hat{\alpha}_t = d^{-1} \text{tr}(\mathbf{W}_t^S)$  and  $\hat{\beta}_t = d^{-1} \text{tr}(\mathbf{W}_t^V)$  across layers, showing that they cluster around the one- and two-parameter  $T \rightarrow \infty$  gradient-flow limit  $(\alpha^*, -\alpha^*)$  (Theorems 6.2–6.3). The normalized traces  $(\hat{\alpha}_t, \hat{\beta}_t)$  on their own do not confirm a full collapse of the form  $(\mathbf{W}_t^S, \mathbf{W}_t^V) \approx (\alpha^* \mathbf{I}, -\alpha^* \mathbf{I})$ , so Figure 3 (Right) displays the whitening diagnostic  $\|\mathbf{X}\mathbf{F}_t^\top/L - \mathbf{I}\|_F/\sqrt{d}$  across layers. In line with (6.1), even these less-restricted models exhibit the same prompt-dependent covariance-whitening as proven earlier for our simpler models.

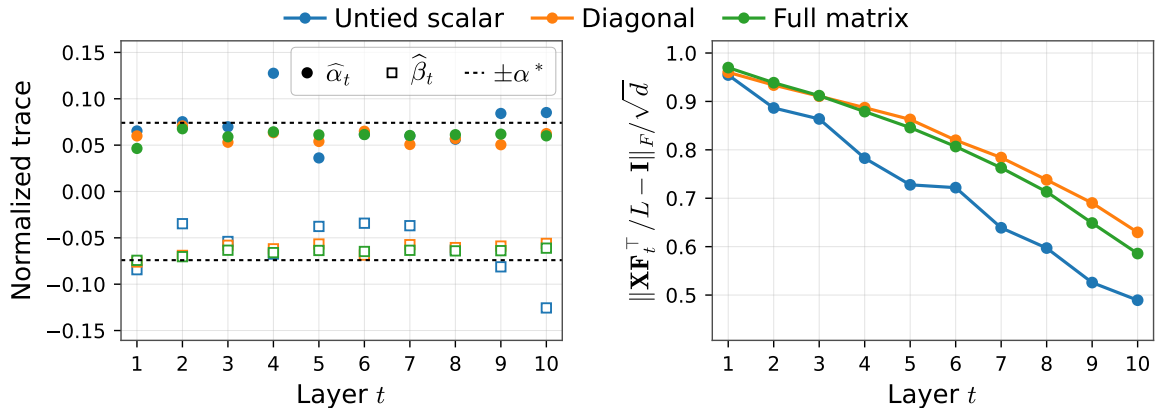


Figure 3: Diagnostics for less-restricted LCA parametrizations (setup same as in Figure 2; see Appendix H). Left: layerwise scalar projections; Right: whitening error across layers.

**Performance of theory-motivated components in standard multi-modal transformers.** We next ask whether the novel theory-motivated components of our CA architecture (Section 5) remain useful after replacing the linearized model with standard transformer blocks—softmax multi-head attention, layer normalization, MLP blocks. We call this architecture—with all the standard transformer blocks on top of our innovations in Section 5—the “full paper-inspired model” (see Appendix I for details). Recall from (5.2)–(5.3) that each layer updates an evolving state  $\mathbf{F}_t$  using two nonstandard ingredients: a CA term  $\mathbf{A}_t$  between

$\mathbf{F}_t$  and the data  $\mathbf{X}$ , and an additional skip term  $\mathbf{S}_t$  which re-injects  $\mathbf{X}$  at every layer. We evaluate on corrupted<sup>2</sup> avMNIST [Vielzeuf et al., 2019], a paired audio-visual digit classification benchmark. We compare the full paper-inspired model against a standard bidirectional CA transformer [Lu et al., 2019] and three ablations: (i) A no-injection ablation removes the  $\mathbf{S}_t$  term from (5.2), while retaining CA between  $\mathbf{F}_t$  and  $\mathbf{X}$ . (ii) A no-CA ablation retains the re-injection term but replaces the  $\mathbf{F}_t$ - $\mathbf{X}$  CA update by self-attention of  $\mathbf{F}_t$  with itself. (iii) The final ablation removes both mechanisms, yielding a conventional self-attention model. Architecture and training details are deferred to Appendix I.

Model	Params	Best test acc. (%)	Best epoch
<b>Full paper-inspired model (Inj. &amp; cross-attn)</b>	$4.36 \times 10^4$	<b>63.85</b>	64
No injection	$3.82 \times 10^4$	62.72	65
No cross-attn	$4.36 \times 10^4$	62.10	79
No inj. & no cross-attn	$3.82 \times 10^4$	60.79	90
Standard bi-CA transformer	$6.07 \times 10^4$	62.72	62

Table 1: Classification results on avMNIST for the full paper-inspired model, three ablations thereof, and a standard bi-directional cross-attention transformer. All models use (pre) layer-norm, 4-headed multi-head attention, 10 attention layers, embedding dim.  $d = 16$ , hidden dim.  $d_h = 32$ , dropout rate of 0.1, GELU MLP blocks, and appended CLS token. Training: cross-entropy loss over 100 epochs using AdamW optimizer with learning rate  $3 \times 10^{-4}$  and weight decay  $10^{-4}$ . Model parameter counts and best test accuracy with corresponding epoch is shown.

Table 1 shows that our full paper-inspired model achieves the best test accuracy among all compared architectures. In particular, it outperforms each ablation. Additionally, it improves over the standard bidirectional cross-attention transformer, a standard fusion architecture for multimodal transformers [Lu et al., 2019], despite the latter having more trainable parameters. These results suggest that both mechanisms identified by our theory—cross-attention between the evolving state  $\mathbf{F}_t$  and the original data  $\mathbf{X}$ , and recurrent re-injection of the covariates through  $\mathbf{S}_t$ —remain useful in more practical deep-learning implementations. While preliminary, the results are promising and motivate further investigation of our architecture in larger-scale multimodal settings.

## 8 Discussion

We studied a multi-modal task in which each prompt is generated by a latent factor model, inducing prompt-dependent covariate statistics which place the setting outside of standard unimodal ICL analyses. To demonstrate this added complexity, we first established the failure of single-layer LSA models standard in the literature. Motivated by this limitation, we introduced a novel transformer-like architecture, incorporating both depth and CA, proving not only its expressibility for the ICL task, but also demonstrating its capacity to learn the Bayes-optimal predictor via gradient flow. To our knowledge, our work is the first to tackle a multi-modal ICL task in a mathematically tractable setting and provably overcome covariate distribution shifts among prompts. While preliminary, our empirical findings (Table 1) demonstrate the promise of our new architectural innovations (Section 5) and motivate, as an important future direction, further empirical studies benchmarking these approaches on larger-scale multi-modal problems. Another important

<sup>2</sup>We add substantial noise to covariates so the task is not saturated; this explains accuracies in the 60% range in Table 1.

future direction would include extending our population loss level analysis to sample-level results, as done earlier for unimodal problems [Lu et al., 2025]. We expect this direction to pose intriguing mathematical challenges—requiring non-trivial developments in random matrix theory.

## Acknowledgments

The authors thank Daniel Hsu for helpful feedback on an earlier version of this manuscript. N.B. acknowledges support from the *Fonds de recherche du Québec—Nature et technologies* (FRQNT). S.S. gratefully acknowledges support from the National Science Foundation (DMS CAREER 2239234), Office of Naval Research (N00014-23-1-2489) and Air Force Office of Scientific Research (FA9950-23-1-0429). P.S. gratefully acknowledges support from the National Science Foundation (DMS CAREER 2440824) and the Office of Naval Research (N00014-26-1-2144).

## References

- Kwangjun Ahn, Xiang Cheng, Hadi Daneshmand, and Suvrit Sra. Transformers learn to implement pre-conditioned gradient descent for in-context learning. In *Thirty-seventh Conference on Neural Information Processing Systems*, 2023.
- Ekin Akyürek, Dale Schuurmans, Jacob Andreas, Tengyu Ma, and Denny Zhou. What learning algorithm is in-context learning? investigations with linear models. In *The Eleventh International Conference on Learning Representations*, 2023.
- Jean-Baptiste Alayrac, Jeff Donahue, Pauline Luc, Antoine Miech, Iain Barr, Yana Hasson, Karel Lenc, Arthur Mensch, Katherine Millican, Malcolm Reynolds, Roman Ring, Eliza Rutherford, Serkan Cabi, Tengda Han, Zhitao Gong, Sina Samangooei, Marianne Monteiro, Jacob Menick, Sebastian Borgeaud, Andrew Brock, Aida Nematzadeh, Sahand Sharifzadeh, Mikolaj Binkowski, Ricardo Barreira, Oriol Vinyals, Andrew Zisserman, and Karen Simonyan. Flamingo: a visual language model for few-shot learning. In Alice H. Oh, Alekh Agarwal, Danielle Belgrave, and Kyunghyun Cho, editors, *Advances in Neural Information Processing Systems*, 2022.
- Luca Arnaboldi, Bruno Loureiro, Ludovic Stephan, Florent Krzakala, and Lenka Zdeborova. Asymptotics of SGD in sequence-single index models and single-layer attention networks. In *The Thirty-ninth Annual Conference on Neural Information Processing Systems*, 2025.
- Yu Bai, Fan Chen, Huan Wang, Caiming Xiong, and Song Mei. Transformers as statisticians: Provable in-context learning with in-context algorithm selection. In *Workshop on Efficient Systems for Foundation Models @ ICML2023*, 2023.
- Nicholas Barnfield, Hugo Cui, and Yue M Lu. High-dimensional analysis of single-layer attention for sparse-token classification. *arXiv preprint arXiv:2509.25153*, 2025.
- Tom Brown, Benjamin Mann, Nick Ryder, Melanie Subbiah, Jared D Kaplan, Prafulla Dhariwal, Arvind Neelakantan, Pranav Shyam, Girish Sastry, Amanda Askell, et al. Language models are few-shot learners. *Advances in neural information processing systems*, 33:1877–1901, 2020.
- Tianxi Cai, Feiqing Huang, Ryumei Nakada, Linjun Zhang, and Doudou Zhou. Contrastive learning on multimodal analysis of electronic health records. *arXiv preprint arXiv:2403.14926*, 2024.

- Siyu Chen, Heejune Sheen, Tianhao Wang, and Zhuoran Yang. Training dynamics of multi-head softmax attention for in-context learning: Emergence, convergence, and optimality. *arXiv preprint arXiv:2402.19442*, 2024.
- Michelle Ching, Ioana Popescu, Nico Smith, Tianyi Ma, William G Underwood, and Richard J Samworth. Efficient and minimax-optimal in-context nonparametric regression with transformers. *arXiv preprint arXiv:2601.15014*, 2026.
- Lenaic Chizat and Francis Bach. On the global convergence of gradient descent for over-parameterized models using optimal transport. *Advances in neural information processing systems*, 31, 2018.
- Haotian Cui, Alejandro Tejada-Lapuerta, Maria Brbić, Julio Saez-Rodriguez, Simona Cristea, Hani Goodarzi, Mohammad Lotfollahi, Fabian J Theis, and Bo Wang. Towards multimodal foundation models in molecular cell biology. *Nature*, 640(8059):623–633, 2025.
- Hugo Cui, Freya Behrens, Florent Krzakala, and Lenka Zdeborová. A phase transition between positional and semantic learning in a solvable model of dot-product attention. *Advances in Neural Information Processing Systems*, 37:36342–36389, 2024.
- Yash Deshpande, Subhabrata Sen, Andrea Montanari, and Elchanan Mossel. Contextual stochastic block models. *Advances in Neural Information Processing Systems*, 31, 2018.
- Daisy Yi Ding, Shuangning Li, Balasubramanian Narasimhan, and Robert Tibshirani. Cooperative learning for multiview analysis. *Proceedings of the National Academy of Sciences*, 119(38):e2202113119, 2022.
- Shivam Garg, Dimitris Tsipras, Percy S Liang, and Gregory Valiant. What can transformers learn in-context? a case study of simple function classes. *Advances in neural information processing systems*, 35: 30583–30598, 2022.
- Karol Gregor and Yann LeCun. Learning fast approximations of sparse coding. In *Proceedings of the 27th international conference on international conference on machine learning*, pages 399–406, 2010.
- Yu Gui, Cong Ma, and Zongming Ma. Multi-modal contrastive learning adapts to intrinsic dimensions of shared latent variables. *arXiv preprint arXiv:2505.12473*, 2025.
- Yu Huang, Yuan Cheng, and Yingbin Liang. In-context convergence of transformers. *arXiv preprint arXiv:2310.05249*, 2023.
- Andrew Jaegle, Felix Gimeno, Andy Brock, Oriol Vinyals, Andrew Zisserman, and Joao Carreira. Perceiver: General perception with iterative attention. In *International conference on machine learning*, pages 4651–4664. PMLR, 2021.
- Christian Keup and Lenka Zdeborová. Optimal thresholds and algorithms for a model of multi-modal learning in high dimensions. *Journal of Statistical Mechanics: Theory and Experiment*, 2025(9):093302, 2025.
- Mary I Letey, Jacob A Zavatone-Veth, Yue M Lu, and Cengiz Pehlevan. Pretrain-test task alignment governs generalization in in-context learning. *arXiv preprint arXiv:2509.26551*, 2025.
- Chunyu Li, Zhe Gan, Zhengyuan Yang, Jianwei Yang, Linjie Li, Lijuan Wang, Jianfeng Gao, et al. Multimodal foundation models: From specialists to general-purpose assistants. *Foundations and Trends® in Computer Graphics and Vision*, 16(1-2):1–214, 2024.

- Yingcong Li, Muhammed Emrullah Ildiz, Dimitris Papailiopoulos, and Samet Oymak. Transformers as algorithms: Generalization and stability in in-context learning. In *International conference on machine learning*, pages 19565–19594. PMLR, 2023.
- Xiaohao Liu, Xiaobo Xia, See-Kiong Ng, and Tat-Seng Chua. Continual multimodal contrastive learning. *arXiv preprint arXiv:2503.14963*, 2025.
- Jiasen Lu, Dhruv Batra, Devi Parikh, and Stefan Lee. Vilbert: Pretraining task-agnostic visiolinguistic representations for vision-and-language tasks. *Advances in neural information processing systems*, 32, 2019.
- Yue M Lu, Mary Letey, Jacob A Zavatore-Veth, Anindita Maiti, and Cengiz Pehlevan. Asymptotic theory of in-context learning by linear attention. *Proceedings of the National Academy of Sciences*, 122(28): e2502599122, 2025.
- Tianyi Ma, Tengyao Wang, and Richard J Samworth. Provable test-time adaptivity and distributional robustness of in-context learning. *arXiv preprint arXiv:2510.23254*, 2025.
- Rodrigo Maulen-Soto, Pierre Marion, and Claire Boyer. Attention-based clustering. In *The Thirty-ninth Annual Conference on Neural Information Processing Systems*, 2025.
- Pierre Mergny and Lenka Zdeborová. Spectral thresholds in correlated spiked models and fundamental limits of partial least squares. *arXiv preprint arXiv:2510.17561*, 2025.
- Vishal Monga, Yuelong Li, and Yonina C Eldar. Algorithm unrolling: Interpretable, efficient deep learning for signal and image processing. *IEEE Signal Processing Magazine*, 38(2):18–44, 2021.
- Sagnik Nandy and Zongming Ma. Multimodal data integration and cross-modal querying via orchestrated approximate message passing. *arXiv preprint arXiv:2407.19030*, 2024.
- Samet Oymak, Ankit Singh Rawat, Mahdi Soltanolkotabi, and Christos Thrampoulidis. On the role of attention in prompt-tuning. In *International Conference on Machine Learning*, pages 26724–26768. PMLR, 2023.
- Alec Radford, Jong Wook Kim, Chris Hallacy, Aditya Ramesh, Gabriel Goh, Sandhini Agarwal, Girish Sastry, Amanda Askell, Pamela Mishkin, Jack Clark, et al. Learning transferable visual models from natural language supervision. In *International conference on machine learning*, pages 8748–8763. PMLR, 2021.
- Andrew M Saxe, James L McClelland, and Surya Ganguli. Exact solutions to the nonlinear dynamics of learning in deep linear neural networks. *arXiv preprint arXiv:1312.6120*, 2013.
- Renat Sergazinov, Armeen Taeb, and Irina Gaynanova. A spectral method for multi-view subspace learning using the product of projections. *Biometrika*, page asaf088, 2025.
- Wei Shen, Ruida Zhou, Jing Yang, and Cong Shen. On the training convergence of transformers for in-context classification of gaussian mixtures. In *Forty-second International Conference on Machine Learning*, 2025.
- Jean-Jacques E Slotine, Weiping Li, et al. *Applied nonlinear control*, volume 199. Prentice hall Englewood Cliffs, NJ, 1991.

- Hao Tan and Mohit Bansal. LXMERT: Learning cross-modality encoder representations from transformers. In *Proceedings of the 2019 Conference on Empirical Methods in Natural Language Processing and the 9th International*, pages 5100–5111. Association for Computational Linguistics, 2019. doi: 10.18653/v1/D19-1514. URL <https://aclanthology.org/D19-1514/>.
- Emanuele Troiani, Hugo Cui, Yatin Dandi, Florent Krzakala, and Lenka Zdeborova. Fundamental limits of learning in sequence multi-index models and deep attention networks: high-dimensional asymptotics and sharp thresholds. In *Forty-second International Conference on Machine Learning*, 2025.
- Ashish Vaswani, Noam Shazeer, Niki Parmar, Jakob Uszkoreit, Llion Jones, Aidan N Gomez, Łukasz Kaiser, and Illia Polosukhin. Attention is all you need. *Advances in neural information processing systems*, 30, 2017.
- Valentin Vielzeuf, Alexis Lechervy, Stéphane Pateux, and Frédéric Jurie. Centralnet: A multilayer approach for multimodal fusion. In Laura Leal-Taixé and Stefan Roth, editors, *Computer Vision – ECCV 2018 Workshops*, pages 575–589, Cham, 2019. Springer International Publishing. ISBN 978-3-030-11024-6.
- Johannes Von Oswald, Eyvind Niklasson, Ettore Randazzo, João Sacramento, Alexander Mordvintsev, Andrey Zhmoginov, and Max Vladymyrov. Transformers learn in-context by gradient descent. In *International Conference on Machine Learning*, pages 35151–35174. PMLR, 2023.
- Zirui Wang, Mengzhou Xia, Luxi He, Howard Chen, Yitao Liu, Richard Zhu, Kaiqu Liang, Xindi Wu, Haotian Liu, Sadhika Malladi, et al. Charxiv: Charting gaps in realistic chart understanding in multimodal llms. *Advances in Neural Information Processing Systems*, 37:113569–113697, 2024.
- Jingfeng Wu, Difan Zou, Zixiang Chen, Vladimir Braverman, Quanquan Gu, and Peter Bartlett. How many pretraining tasks are needed for in-context learning of linear regression? In *The Twelfth International Conference on Learning Representations*, 2024.
- Sang Michael Xie, Aditi Raghunathan, Percy Liang, and Tengyu Ma. An explanation of in-context learning as implicit bayesian inference. In *International Conference on Learning Representations*, 2022.
- Ruibin Xiong, Yunchang Yang, Di He, Kai Zheng, Shuxin Zheng, Chen Xing, Huishuai Zhang, Yanyan Lan, Liwei Wang, and Tiejian Liu. On layer normalization in the transformer architecture. In *International conference on machine learning*, pages 10524–10533. PMLR, 2020.
- Xiaodong Yang, Buyu Lin, and Subhabrata Sen. Fundamental limits of community detection from multi-view data: multi-layer, dynamic and partially labeled block models. *The Annals of Statistics*, 53(6):2728–2756, 2025.
- Ruiqi Zhang, Spencer Frei, and Peter L Bartlett. Trained transformers learn linear models in-context. *Journal of Machine Learning Research*, 25(49):1–55, 2024a.
- Ruiqi Zhang, Jingfeng Wu, and Peter Bartlett. In-context learning of a linear transformer block: Benefits of the MLP component and one-step GD initialization. In *The Thirty-eighth Annual Conference on Neural Information Processing Systems*, 2024b.
- Yedi Zhang, Aaditya K Singh, Peter E. Latham, and Andrew M Saxe. Training dynamics of in-context learning in linear attention. In *Forty-second International Conference on Machine Learning*, 2025.

# A Notation, basic identities, and the Bayes-predictor

## A.1 Notation and conventions

We work with a single prompt (task) unless otherwise stated. For two sequences  $(a_n)_{n \geq 1}$  and  $(b_n)_{n \geq 1}$ , we write

$$a_n = O(b_n)$$

to mean  $a_n \leq C \cdot b_n$  for some constant  $C > 0$  for  $n$  sufficiently large. We also use  $o(1)$  to denote a sequence of terms which vanish as the ambient index grows. For example, writing  $a_n = o(1)$  implies  $a_n \rightarrow 0$  as  $n \rightarrow \infty$ .

Symbol	Meaning
$d = d_1 + d_2$	total covariate dimension
$L$	context length (we use $L_{\text{tr}}$ or $L_{\text{te}}$ when needed)
$\mathbf{x}_i \in \mathbb{R}^d$	stacked covariate for context token $i \in [L]$
$\mathbf{x}_q \in \mathbb{R}^d$	query covariate
$y_i \in \mathbb{R}$	context response for token $i \in [L]$
$y_q \in \mathbb{R}$	query response
$\mathbf{m} \in \mathbb{R}^d$	stacked modality vector (prompt-specific), $\mathbf{m} = [v; r]$
$\zeta \in \mathbb{R}$	prompt-specific scalar controlling the response
$u_i \sim \mathcal{N}(0, 1)$	latent scalar shared across modalities and response
$\boldsymbol{\mu}_i \sim \mathcal{N}(0, \mathbf{I}_d)$	stacked noise in covariates
$\boldsymbol{\Lambda} = \mathbf{I} + \mathbf{m}\mathbf{m}^\top$	covariate covariance conditional on $\mathbf{m}$
$\boldsymbol{\Sigma}$	joint covariance of $(x, y)$ conditioned on $(\mathbf{m}, \zeta)$
$Z := 1 + \ \mathbf{m}\ ^2$	top eigenvalue of $\boldsymbol{\Lambda}$ (rank-one spike)
$\mathbf{w} \in \mathbb{R}^d$	Bayes-optimal regression coefficient: $\mathbf{w} = \frac{\zeta}{1 + \ \mathbf{m}\ ^2} \mathbf{m}$
$\underline{m}, \bar{m}$	$\underline{m} = \text{ess inf } \ \mathbf{m}\ ^2$ , $\bar{m} = \text{ess sup } \ \mathbf{m}\ ^2$
$\underline{Z}, \bar{Z}$	$\underline{Z} = 1 + \underline{m}$ , $\bar{Z} = 1 + \bar{m} = \text{ess sup } Z$

## A.2 Joint Gaussian form and Bayes-predictor

Recall the data generating process (Section 3): for  $i \in [L] \cup \{q\}$ ,

$$\mathbf{x}_i = u_i \mathbf{m} + \boldsymbol{\mu}_i, \quad y_i = \zeta u_i,$$

with  $u_i \sim \mathcal{N}(0, 1)$  and  $\boldsymbol{\mu}_i = [\boldsymbol{\xi}_i, \boldsymbol{\eta}_i] \sim \mathcal{N}(0, \mathbf{I}_d)$  independent across tokens  $i$  and independent of  $(\mathbf{m}, \zeta)$ .

**Lemma A.1** (Joint covariance and Bayes coefficient). *Conditional on  $(\mathbf{m}, \zeta)$ , the pair  $(\mathbf{x}_i, y_i) \in \mathbb{R}^{d+1}$  is jointly Gaussian with mean 0 and covariance*

$$\boldsymbol{\Sigma} = \begin{bmatrix} \boldsymbol{\Lambda} & \zeta \mathbf{m} \\ \zeta \mathbf{m}^\top & \zeta^2 \end{bmatrix}, \quad \boldsymbol{\Lambda} = \mathbf{I} + \mathbf{m}\mathbf{m}^\top.$$

Moreover,

$$\mathbb{E}[y_i \mid \mathbf{m}, \zeta, \mathbf{x}_i] = \mathbf{w}^\top \mathbf{x}_i, \quad \mathbf{w} = \frac{\zeta}{1 + \|\mathbf{m}\|^2} \mathbf{m},$$

and we may write

$$y_i = \langle \mathbf{w}, \mathbf{x}_i \rangle + \varepsilon_i, \quad \varepsilon_i \perp \mathbf{x}_i \mid (\mathbf{m}, \zeta), \quad \varepsilon_i \sim \mathcal{N}\left(0, \frac{\zeta^2}{1 + \|\mathbf{m}\|^2}\right).$$

*Proof.* We compute conditional covariances given  $(\mathbf{m}, \zeta)$ :

$$\boldsymbol{\Sigma}_{x,x} := \mathbb{E}[\mathbf{x}_i \mathbf{x}_i^\top \mid \mathbf{m}, \zeta] = \mathbb{E}[(u_i \mathbf{m} + \boldsymbol{\mu}_i)(u_i \mathbf{m} + \boldsymbol{\mu}_i)^\top] = \mathbf{m} \mathbf{m}^\top + \mathbf{I} = \boldsymbol{\Lambda},$$

$$\boldsymbol{\Sigma}_{x,y} := \mathbb{E}[\mathbf{x}_i y_i \mid \mathbf{m}, \zeta] = \mathbb{E}[(u_i \mathbf{m} + \boldsymbol{\mu}_i) \cdot \zeta u_i] = \zeta \mathbb{E}[u_i^2] \mathbf{m} = \zeta \mathbf{m},$$

$$\boldsymbol{\Sigma}_{y,y} := \mathbb{E}[y_i^2 \mid \mathbf{m}, \zeta] = \zeta^2 \mathbb{E}[u_i^2] = \zeta^2,$$

yielding the stated  $\boldsymbol{\Sigma}$ . For a jointly Gaussian vector, the conditional mean is

$$\mathbb{E}[y_i \mid \mathbf{x}_i, \mathbf{m}, \zeta] = \boldsymbol{\Sigma}_{x,y}^\top \boldsymbol{\Sigma}_{x,x}^{-1} \mathbf{x}_i = (\zeta \mathbf{m})^\top \boldsymbol{\Lambda}^{-1} \mathbf{x}_i$$

and so  $\mathbf{w} = \boldsymbol{\Lambda}^{-1}(\zeta \mathbf{m})$ . Using the Sherman–Morrison formula,

$$\boldsymbol{\Lambda}^{-1} = (\mathbf{I} + \mathbf{m} \mathbf{m}^\top)^{-1} = \mathbf{I} - \frac{\mathbf{m} \mathbf{m}^\top}{1 + \|\mathbf{m}\|^2}.$$

and hence,

$$\mathbf{w} = \left( \mathbf{I} - \frac{\mathbf{m} \mathbf{m}^\top}{1 + \|\mathbf{m}\|^2} \right) \zeta \mathbf{m} = \zeta \mathbf{m} - \zeta \frac{\|\mathbf{m}\|^2}{1 + \|\mathbf{m}\|^2} \mathbf{m} = \frac{\zeta}{1 + \|\mathbf{m}\|^2} \mathbf{m}.$$

Finally, the conditional variance of  $y_i$  given  $\mathbf{x}_i$  is

$$\begin{aligned} \text{Var}(y_i \mid \mathbf{x}_i, \mathbf{m}, \zeta) &= \boldsymbol{\Sigma}_{y,y} - \boldsymbol{\Sigma}_{x,y}^\top \boldsymbol{\Sigma}_{x,x}^{-1} \boldsymbol{\Sigma}_{x,y} \\ &= \zeta^2 - (\zeta \mathbf{m})^\top \boldsymbol{\Lambda}^{-1} (\zeta \mathbf{m}) \\ &= \zeta^2 (1 - \|\mathbf{m}\|^2 / (1 + \|\mathbf{m}\|^2)) \\ &= \zeta^2 / (1 + \|\mathbf{m}\|^2). \end{aligned}$$

The residual  $\varepsilon_i := y_i - \langle \mathbf{w}, \mathbf{x}_i \rangle$  is independent of  $\mathbf{x}_i$  conditional on  $(\mathbf{m}, \zeta)$  by Gaussianity.  $\square$

### A.3 Law of large numbers for prompt statistics

Let  $\mathbf{X} = [\mathbf{x}_1, \dots, \mathbf{x}_L] \in \mathbb{R}^{d \times L}$  and  $\mathbf{y} = [y_1, \dots, y_L]^\top \in \mathbb{R}^L$  denote the covariate matrix and target vector, and define the context sample covariance

$$\widehat{\boldsymbol{\Lambda}} := \frac{1}{L} \mathbf{X} \mathbf{X}^\top.$$

**Lemma A.2** (Matrix LLN at fixed dimension). *Fix  $(\mathbf{m}, \zeta)$  and thus  $\boldsymbol{\Lambda} = \mathbf{I} + \mathbf{m} \mathbf{m}^\top$ . Then, almost surely as  $L \rightarrow \infty$ ,*

$$\widehat{\boldsymbol{\Lambda}} \rightarrow \boldsymbol{\Lambda}$$

*entry-wise, and hence also in operator norm. Moreover,*

$$\frac{1}{L} \mathbf{X} \mathbf{y} \rightarrow \mathbb{E}[\mathbf{x}_i y_i \mid \mathbf{m}, \zeta] = \zeta \mathbf{m}, \quad \frac{1}{L} \sum_{i=1}^L y_i^2 \rightarrow \mathbb{E}[y_i^2 \mid \mathbf{m}, \zeta] = \zeta^2.$$

*Finally, writing  $y_i = \langle \mathbf{w}, \mathbf{x}_i \rangle + \varepsilon_i$  as in Lemma A.1 and letting  $\boldsymbol{\varepsilon} = (\varepsilon_1, \dots, \varepsilon_L)^\top$ ,*

$$\frac{1}{L} \mathbf{X} \boldsymbol{\varepsilon} \rightarrow \mathbf{0} \quad \text{almost surely.}$$

*Proof.* Conditional on  $(\mathbf{m}, \zeta)$ , the pairs  $(\mathbf{x}_i, y_i)$  are i.i.d. Gaussian with finite second moments, so the stated convergences follow from the law of large numbers entrywise.  $\square$

## B Proof of Theorem 4.1

Recall the single-layer LSA predictor

$$\hat{y}_q = \text{LSA}(\mathbf{E}_X; \theta)_{d+1, L+1}, \quad \text{LSA}(\mathbf{E}_X; \theta) = \mathbf{E}_X + \mathbf{W}_{PV} \mathbf{E}_X \cdot \frac{\mathbf{E}_X^\top \mathbf{W}_{KQ} \mathbf{E}_X}{L},$$

where

$$\mathbf{E}_X = \begin{bmatrix} \mathbf{X} & \mathbf{x}_q \\ \mathbf{y}^\top & 0 \end{bmatrix} \in \mathbb{R}^{(d+1) \times (L+1)}.$$

We provide the full proof of Theorem 4.1 below.

*Proof of Theorem 4.1.* Let us write the weight matrix  $\mathbf{W}_{KQ}$  in block form

$$\mathbf{W}_{KQ} = \begin{bmatrix} \mathbf{A} & \mathbf{b}' \\ \mathbf{b}^\top & c \end{bmatrix}, \quad \mathbf{A} \in \mathbb{R}^{d \times d}, \mathbf{b}, \mathbf{b}' \in \mathbb{R}^d, c \in \mathbb{R},$$

and denote the last row of  $\mathbf{W}_{PV}$  by

$$\begin{bmatrix} \mathbf{u}^\top & v \end{bmatrix} := \mathbf{e}_{d+1}^\top \mathbf{W}_{PV}, \quad \mathbf{u} \in \mathbb{R}^d, v \in \mathbb{R}.$$

Since  $(\mathbf{E}_X)_{d+1, L_{te}+1} = 0$ , the residual term (skip-connection) in  $\text{LSA}(\mathbf{E}_X; \theta)$  does not contribute to the predictor  $\hat{y}_q$  and so

$$\hat{y}_q = \mathbf{e}_{d+1}^\top \mathbf{W}_{PV} \mathbf{E}_X \cdot \frac{\mathbf{E}_X^\top \mathbf{W}_{KQ} \mathbf{E}_X}{L_{te}} \mathbf{e}_{L_{te}+1}.$$

For  $i \in [L_{te}]$ , the  $i$ -th entry of the vector  $\mathbf{E}_X^\top \mathbf{W}_{KQ} \mathbf{E}_X \mathbf{e}_{L_{te}+1}$  is given by

$$[\mathbf{E}_X^\top \mathbf{W}_{KQ} \mathbf{E}_X \mathbf{e}_{L_{te}+1}]_i = \begin{bmatrix} \mathbf{x}_i \\ y_i \end{bmatrix}^\top \begin{bmatrix} \mathbf{A} & \mathbf{b}' \\ \mathbf{b}^\top & c \end{bmatrix} \begin{bmatrix} \mathbf{x}_q \\ 0 \end{bmatrix} = (\mathbf{x}_i^\top \mathbf{A} \mathbf{x}_q + y_i \mathbf{b}^\top \mathbf{x}_q).$$

Moreover, the  $(L_{te}+1)$ -th entry of  $\frac{1}{L_{te}} \mathbf{E}_X^\top \mathbf{W}_{KQ} \mathbf{E}_X \mathbf{e}_{L_{te}+1}$  is of order  $O(\frac{1}{L_{te}})$  and thus negligible as  $L_{te} \rightarrow \infty$ . Hence, we obtain

$$\hat{y}_q = \frac{1}{L_{te}} \sum_{i=1}^{L_{te}} (\mathbf{u}^\top \mathbf{x}_i + v y_i) (\mathbf{x}_i^\top \mathbf{A} + y_i \mathbf{b}^\top) \mathbf{x}_q + o(1). \quad (\text{B.1})$$

Conditioned on  $(\mathbf{m}, \zeta)$ , the context tokens  $\{(\mathbf{x}_i, y_i)\}_{i=1}^{L_{te}}$  are i.i.d., and  $\mathbf{x}_q$  is independent of  $\{(\mathbf{x}_i, y_i)\}_{i=1}^{L_{te}}$  with the same conditional law as  $\mathbf{x}_i$ . Applying Lemma A.2 to each empirical moment that appears when expanding (B.1) yields, almost surely (for fixed  $(\mathbf{m}, \zeta, \mathbf{x}_q)$ ),

$$\hat{y}_q \rightarrow \langle \hat{\mathbf{w}}, \mathbf{x}_q \rangle,$$

as  $L_{te} \rightarrow \infty$  where the limiting regression vector  $\hat{\mathbf{w}} = \hat{\mathbf{w}}(\mathbf{m}, \zeta) \in \mathbb{R}^d$  is

$$\hat{\mathbf{w}}(\mathbf{m}, \zeta)^\top = \mathbf{u}^\top \mathbf{\Lambda} \mathbf{A} + \left( (\mathbf{u}^\top \mathbf{m}) \mathbf{b}^\top + v \mathbf{m}^\top \mathbf{A} \right) \zeta + v \mathbf{b}^\top \zeta^2. \quad (\text{B.2})$$

We now show that  $\mathbb{P}(\hat{\mathbf{w}}(\mathbf{m}, \zeta) = \mathbf{w}(\mathbf{m}, \zeta)) = 0$ . We begin by assuming, for contradiction, that indeed  $\langle \hat{\mathbf{w}}, \mathbf{x}_q \rangle = \langle \mathbf{w}, \mathbf{x}_q \rangle$  and then examine the measure of this event. Since  $\mathbf{x}_q | (\mathbf{m}, \zeta) \sim \mathcal{N}(0, \mathbf{\Lambda})$ , we must have  $\hat{\mathbf{w}}(\mathbf{m}, \zeta) = \mathbf{w}(\mathbf{m}, \zeta)$ . Note that the Bayes vector  $\mathbf{w}$  is linear in  $\zeta$ , while, in contrast,  $\hat{\mathbf{w}}(\mathbf{m}, \zeta)$  in (B.2) is a polynomial in  $\zeta$  of degree two and so the  $\zeta^2$ -coefficient must vanish:  $v \mathbf{b} = \mathbf{0}_d$ . Similarly, since  $\mathbf{w}$  has no constant ( $\zeta^0$ ) term, we must have  $\mathbf{A}^\top \mathbf{\Lambda} \mathbf{u} = \mathbf{0}_d$ . It then follows that

$$\hat{\mathbf{w}}(\mathbf{m}, \zeta)^\top = \mathbf{m}^\top \mathbf{B} \zeta \quad (\text{B.3})$$

for the fixed matrix  $\mathbf{B} = \mathbf{u}\mathbf{b}^\top + v\mathbf{A}$ . Recalling that

$$\mathbf{w} = \frac{\zeta}{1 + \|\mathbf{m}\|^2} \mathbf{m},$$

by transposing (B.3), it follows that  $(1 + \|\mathbf{m}\|^2)^{-1}$  is an eigenvalue of  $\mathbf{B}^\top$ , equivalently of  $\mathbf{B}$ . Since  $\|\mathbf{m}\|$  is atomless while the spectrum of  $\mathbf{B}$  is finite, this cannot occur—explicitly,

$$\sup_{\mathbf{B} \in \mathbb{R}^{d \times d}} \mathbb{P} \left( \frac{1}{1 + \|\mathbf{m}\|^2} \in \sigma(\mathbf{B}) \right) = 0$$

where  $\sigma(\mathbf{B})$  denotes the spectrum of  $\mathbf{B}$ . Hence,

$$\mathbb{P}(\hat{\mathbf{w}}(\mathbf{m}, \zeta) = \mathbf{w}(\mathbf{m}, \zeta)) = 0$$

which establishes the desired result. □

## C CA algebra and preliminaries

This appendix collects algebraic identities for the LCA stack and the final LSA readout. These identities are used in the proofs of Theorems 6.2 and 6.3.

### C.1 LSA readout with frozen parameters

Taking inspiration from the initialization strategy of Zhang et al. [2024a], we initialize the  $\mathbf{W}^{PV}$  and  $\mathbf{W}^{KQ}$  by

$$\mathbf{W}^{PV} = \begin{bmatrix} \mathbf{0}_{d \times d} & \mathbf{0}_d \\ \mathbf{0}_d^\top & 1 \end{bmatrix}, \quad \mathbf{W}^{KQ} = \begin{bmatrix} \mathbf{I}_d & \mathbf{0}_d \\ \mathbf{0}_d^\top & 0 \end{bmatrix}.$$

**Lemma C.1** (Closed-form readout). *With the above  $\mathbf{W}^{PV}, \mathbf{W}^{KQ}$ , the single-layer LSA readout satisfies*

$$\hat{\mathbf{y}}_q = \text{LSA}(\mathbf{E}_F)_{d+1, L+1} = \mathbf{w}^\top \left[ \frac{1}{L} \sum_{i=1}^L \mathbf{x}_i \mathbf{f}_i^\top \right] \mathbf{x}_q + \left[ \frac{1}{L} \sum_{i=1}^L \varepsilon_i \mathbf{f}_i^\top \right] \mathbf{x}_q.$$

and

$$\left[ \frac{1}{L} \sum_{i=1}^L \varepsilon_i \mathbf{f}_i^\top \right] \mathbf{x}_q \rightarrow 0$$

almost surely as  $L \rightarrow \infty$  if  $\sup_{i \geq 1} \|\mathbf{f}_i\| < \infty$ .

*Proof.* By definition,

$$\text{LSA}(\mathbf{E}_F) = \mathbf{E}_F + \mathbf{W}^{PV} \mathbf{E}_F \cdot \frac{\mathbf{E}_F^\top \mathbf{W}^{KQ} \mathbf{E}_F}{L}.$$

Since  $(\mathbf{E}_F)_{d+1,L+1} = 0$ , given the definitions of  $\mathbf{W}^{PV}$  and  $\mathbf{W}^{KQ}$ , we have

$$\begin{aligned}
\hat{y}_q &= \mathbf{e}_{d+1}^\top \mathbf{W}^{PV} \mathbf{E}_F \cdot \frac{\mathbf{E}_F^\top \mathbf{W}^{KQ} \mathbf{E}_F}{L} \mathbf{e}_{L+1} \\
&= \mathbf{e}_{d+1}^\top \frac{\mathbf{E}_F \mathbf{E}_F^\top}{L} \begin{bmatrix} \mathbf{x}_q \\ 0 \end{bmatrix} \\
&= \mathbf{e}_{d+1}^\top \frac{1}{L} \begin{bmatrix} \mathbf{F} \mathbf{F}^\top + \mathbf{x}_q \mathbf{x}_q^\top & \mathbf{F} \mathbf{y} \\ \mathbf{y}^\top \mathbf{F}^\top & \mathbf{y}^\top \mathbf{y} \end{bmatrix} \begin{bmatrix} \mathbf{x}_q \\ 0 \end{bmatrix} \\
&= \frac{\mathbf{y}^\top \mathbf{F}^\top \mathbf{x}_q}{L} \\
&= \mathbf{w}^\top \left[ \frac{1}{L} \sum_{i=1}^L \mathbf{x}_i \mathbf{f}_i^\top \right] \mathbf{x}_q + \left[ \frac{1}{L} \sum_{i=1}^L \varepsilon_i \mathbf{f}_i^\top \right] \mathbf{x}_q.
\end{aligned}$$

Hence, since  $\mathbb{E}[\varepsilon_i] = 0$  and  $\varepsilon_i \perp \mathbf{f}_i$  as  $\mathbf{F}$  depends only on  $\mathbf{X}$ , the law of large numbers yields

$$\left[ \frac{1}{L} \sum_{i=1}^L \varepsilon_i \mathbf{f}_i^\top \right] \mathbf{x}_q \rightarrow 0$$

almost surely as  $L \rightarrow \infty$ . □

Recall now that  $\mathbf{F}$  and hence  $\{\mathbf{f}_i\}_{i \geq 1}$  depend on the model depth  $T$ . From Lemma C.1, we see that if

$$\frac{1}{L} \mathbf{X} \mathbf{F}^\top \rightarrow \mathbf{I}_d$$

as  $T \rightarrow \infty$ , the asymptotic model predictor will be

$$\lim_{T \rightarrow \infty} \lim_{L \rightarrow \infty} \hat{y}_q = \langle \mathbf{w}, \mathbf{x}_q \rangle,$$

hence yielding the Bayes-optimal prediction. This will be the key step in establishing Theorems 6.2(3) and 6.3(3).

## C.2 Solving the CA recurrence

In the one- and two-scalar simplification, we take (for all layers)

$$\mathbf{W}^K = \mathbf{W}^Q = \mathbf{I}_d, \quad \mathbf{W}^S = \alpha \mathbf{I}_d, \quad \mathbf{W}^V = \beta \mathbf{I}_d,$$

where  $\alpha, \beta \in \mathbb{R}$  are scalar parameters (with the one-parameter model corresponding to  $\beta = -\alpha$ ). Layer-wise, the model then becomes, for  $t = 1, \dots, T$ ,

$$\mathbf{F}_t = \mathbf{F}_{t-1} + \alpha \mathbf{X} + \frac{\beta}{L} \mathbf{X} \mathbf{X}^\top \mathbf{F}_{t-1},$$

with  $\mathbf{F}_0 = \mathbf{0}_{d \times L}$  and  $\mathbf{F} = \mathbf{F}_T$ . Define the sample covariance  $\hat{\mathbf{\Lambda}} := \frac{1}{L} \mathbf{X} \mathbf{X}^\top$ . The following result yields a closed-form expression for the final output of the CA stack and establishes the parameter window for which one obtains the Bayes-predictor.

**Lemma C.2.** *The output of the final layer of the CA network is*

$$\mathbf{F} = \mathbf{F}_T = \alpha \sum_{k=0}^{T-1} \mathbf{M}^k \mathbf{X} \quad \text{where} \quad \mathbf{M} = \mathbf{I} + \beta \hat{\mathbf{\Lambda}}.$$

and, for  $\beta \neq 0$ ,

$$\frac{1}{L} \mathbf{X} \mathbf{F}^\top = \frac{\alpha}{\beta} \left[ (\mathbf{I} + \beta \widehat{\boldsymbol{\Lambda}})^T - \mathbf{I} \right].$$

If  $\alpha = -\beta \in (0, 2/(1 + \overline{m}))$ , then as context length  $L \rightarrow \infty$  followed by the number of layers  $T \rightarrow \infty$ , we have

$$\frac{1}{L} \mathbf{X} \mathbf{F}^\top \rightarrow \mathbf{I}.$$

almost surely.

*Proof.* We prove the first statement by induction. For the base case  $T = 1$ , we have trivially  $\mathbf{F}_1 = \alpha \mathbf{X}$  since  $\mathbf{F}_0 = \mathbf{0}_{d \times L}$ . Now, suppose  $\mathbf{F}_{T-1} = \alpha \sum_{k=0}^{T-2} \mathbf{M}^k \mathbf{X}$ . Then,

$$\begin{aligned} \mathbf{F}_T &= \mathbf{F}_{T-1} + \alpha \mathbf{X} + \beta \widehat{\boldsymbol{\Lambda}} \mathbf{F}_{T-1} \\ &= \alpha \mathbf{X} + (\mathbf{I} + \beta \widehat{\boldsymbol{\Lambda}}) \mathbf{F}_{T-1} \\ &= \alpha \mathbf{X} + \alpha \mathbf{M} \sum_{k=0}^{T-2} \mathbf{M}^k \mathbf{X} \\ &= \alpha \mathbf{X} + \alpha \sum_{k=1}^{T-1} \mathbf{M}^k \mathbf{X} = \alpha \sum_{k=0}^{T-1} \mathbf{M}^k \mathbf{X} \end{aligned}$$

which completes the induction. As  $\mathbf{M}$  is symmetric and  $\widehat{\boldsymbol{\Lambda}} = \beta^{-1}(\mathbf{M} - \mathbf{I})$ , a simple computation then yields

$$\begin{aligned} \frac{1}{L} \mathbf{X} \mathbf{F}^\top &= \alpha \widehat{\boldsymbol{\Lambda}} \sum_{k=0}^{T-1} \mathbf{M}^k = \frac{\alpha}{\beta} \sum_{k=0}^{T-1} (\mathbf{M}^{k+1} - \mathbf{M}^k) \\ &= \frac{\alpha}{\beta} (\mathbf{M}^T - \mathbf{I}) = \frac{\alpha}{\beta} \left[ (\mathbf{I} + \beta \widehat{\boldsymbol{\Lambda}})^T - \mathbf{I} \right]. \end{aligned}$$

Now, if  $\alpha = -\beta$ , we have

$$\frac{1}{L} \mathbf{X} \mathbf{F}^\top = \mathbf{I} - (\mathbf{I} - \alpha \widehat{\boldsymbol{\Lambda}})^T \rightarrow \mathbf{I} - (\mathbf{I} - \alpha \boldsymbol{\Lambda})^T$$

as  $L \rightarrow \infty$  by the Law of Large Numbers. As  $\boldsymbol{\Lambda} = \mathbf{I} + \mathbf{m} \mathbf{m}^\top$ , the eigenvalues of  $\mathbf{I} - \alpha \boldsymbol{\Lambda}$  are  $1 - \alpha$  and  $1 - \alpha(1 + \|\mathbf{m}\|^2)$ . Hence, for the choice of  $\alpha \in (0, 2/(1 + \overline{m}))$ , it follows that the operator norm  $\|\mathbf{I} - \alpha \boldsymbol{\Lambda}\| < 1$  almost surely and so  $(\mathbf{I} - \alpha \boldsymbol{\Lambda})^T \rightarrow \mathbf{0}_{d \times d}$  as  $T \rightarrow \infty$  almost surely.  $\square$

*Remark C.3.* From the proof of Lemma C.2, we see that at asymptotic context length the error away from the Bayes-optimal prediction decays geometrically in depth  $T$  so long as the model parameters satisfy  $\alpha = -\beta \in (0, 2/(1 + \overline{m}))$ . Hence, although the result concerns the behavior at infinite depth, in practice small to moderate depth networks should suffice for accurate in-context predictions. This intuition is supported by numerical experiments in Section 7.

## D Proof of Theorem 6.2

This appendix proves Theorem 6.2 for the one-parameter model, i.e. the simplified CA stack with  $\beta = -\alpha$  trained by gradient flow on the limiting population loss. Throughout, we assume Assumption 6.1:  $\|\mathbf{m}\|^2$  is almost surely bounded and has non-degenerate continuous support. Define

$$Z := 1 + \|\mathbf{m}\|^2, \quad \underline{Z} := \text{ess inf } Z, \quad \overline{Z} := \text{ess sup } Z,$$

so  $1 \leq \underline{Z} < \overline{Z} < \infty$ . We begin by determining a simplified form for the loss  $\ell(\alpha)$  and collecting some of its properties.

**Lemma D.1** (One-parameter loss). *The loss  $\ell(\alpha)$  has the form*

$$\ell(\alpha) = \mathbb{E} \left[ \frac{Z-1}{Z} (1 - \alpha Z)^{2T} \right]$$

up to the additive constant  $\mathbb{E}[1/Z]$ , where  $Z = 1 + \|\mathbf{m}\|^2$ . Moreover, the loss has the following properties:

1.  $\ell(\alpha)$  is strictly convex and coercive in the sense that

$$\lim_{|\alpha| \rightarrow \infty} \ell(\alpha) = \infty;$$

2.  $\ell(\alpha)$  has a unique minimizer which lies in  $(0, 1)$ .

*Proof.* By Lemma C.2, the model output can be written as

$$\hat{y}_q = \mathbf{w}^\top (\mathbf{I} - \mathbf{M}^T) \mathbf{x}_q + \frac{1}{L} \boldsymbol{\varepsilon}^\top \mathbf{F}^\top \mathbf{x}_q = \mathbf{w}^\top \mathbf{x}_q - \mathbf{w}^\top \mathbf{M}^T \mathbf{x}_q + \frac{1}{L} \boldsymbol{\varepsilon}^\top \mathbf{F}^\top \mathbf{x}_q.$$

where  $\mathbf{M} = \mathbf{I} - \alpha \hat{\boldsymbol{\Lambda}}$  and  $\hat{\boldsymbol{\Lambda}}$  is the sample covariance matrix with the true covariance being  $\boldsymbol{\Lambda} = \mathbf{I} + \mathbf{m} \mathbf{m}^\top$ .

We begin by conditioning on  $\boldsymbol{\Lambda}$  so that  $\mathbf{x}_i \stackrel{\text{i.i.d.}}{\sim} \mathcal{N}(0, \boldsymbol{\Lambda})$  and  $\mathbf{w} \perp \mathbf{X}, \mathbf{x}_q$ . Then, set  $\sigma^2 := \mathbb{E}[\varepsilon_i^2 | \boldsymbol{\Lambda}]$  and  $\boldsymbol{\Sigma}_w := \text{Cov}(\mathbf{w} | \boldsymbol{\Lambda})$ . Notice that

$$y_q - \hat{y}_q = \mathbf{w}^\top \mathbf{M}^T \mathbf{x}_q + \varepsilon_q - \frac{1}{L} \boldsymbol{\varepsilon}^\top \mathbf{F}^\top \mathbf{x}_q.$$

Let  $\ell(\alpha | \boldsymbol{\Lambda})$  denote the loss  $\ell(\alpha)$  where one conditions on  $\boldsymbol{\Lambda}$ . We have

$$\begin{aligned} \ell(\alpha | \boldsymbol{\Lambda}) &= \mathbb{E}[(\mathbf{w}^\top \mathbf{M}^T \mathbf{x}_q)^2 | \boldsymbol{\Lambda}] + \frac{1}{L^2} \mathbb{E}[(\boldsymbol{\varepsilon}^\top \mathbf{F}^\top \mathbf{x}_q)^2 | \boldsymbol{\Lambda}] + \mathbb{E}[\varepsilon_q^2 | \boldsymbol{\Lambda}] \\ &= \mathbb{E}[\text{tr}(\boldsymbol{\Sigma}_w \mathbf{M}^T \boldsymbol{\Lambda} \mathbf{M}^T) | \boldsymbol{\Lambda}] + \frac{1}{L^2} \mathbb{E}[\sigma^2 \text{tr}(\boldsymbol{\Lambda} \mathbf{F} \mathbf{F}^\top) | \boldsymbol{\Lambda}] + \mathbb{E}[\varepsilon_q^2 | \boldsymbol{\Lambda}] \\ &= \mathbb{E}[\text{tr}(\boldsymbol{\Sigma}_w \boldsymbol{\Lambda} \mathbf{M}^{2T}) | \boldsymbol{\Lambda}] + \frac{\alpha^2}{L} \mathbb{E}[\sigma^2 \text{tr}(\boldsymbol{\Lambda} (\sum_{k=0}^{T-1} \mathbf{M}^k (\mathbf{I} - \mathbf{M}^T))] | \boldsymbol{\Lambda}] + \mathbb{E}[\varepsilon_q^2 | \boldsymbol{\Lambda}]. \end{aligned}$$

In the first line above, the cross-terms vanish after conditioning on  $(\mathbf{m}, \zeta)$ , since  $\boldsymbol{\varepsilon}, \varepsilon_q$  are mean-zero and independent of  $\mathbf{X}, \mathbf{x}_q$ . As the training context length grows, we have

$$\ell(\alpha | \boldsymbol{\Lambda}) := \lim_{L \rightarrow \infty} \ell(\alpha | \boldsymbol{\Lambda}) = \mathbb{E}[\text{tr}(\boldsymbol{\Sigma}_w \boldsymbol{\Lambda} (\mathbf{I} - \alpha \boldsymbol{\Lambda})^{2T}) | \boldsymbol{\Lambda}] + \mathbb{E}[\varepsilon_q^2 | \boldsymbol{\Lambda}]$$

as

$$\frac{\alpha^2}{L} \mathbb{E}[\sigma^2 \text{tr}(\boldsymbol{\Lambda} (\sum_{k=0}^{T-1} \mathbf{M}^k (\mathbf{I} - \mathbf{M}^T))] | \boldsymbol{\Lambda}] \rightarrow 0 \quad \text{as } L \rightarrow \infty$$

since  $\mathbf{M} \in \mathbb{R}^{d \times d}$  and we are holding the embedding dimension  $d$  fixed. Let us write the eigen-decomposition  $\boldsymbol{\Lambda} = \mathbf{U} \boldsymbol{\Gamma} \mathbf{U}^\top$  where  $\mathbf{U}$  is an orthogonal matrix and  $\boldsymbol{\Gamma} = \text{diag}(\gamma_1, \dots, \gamma_d)$  with  $\gamma_i \geq 0$  the eigenvalues of  $\boldsymbol{\Lambda}$ . Writing  $\mathbf{V} = \mathbf{U}^\top \boldsymbol{\Sigma}_w \mathbf{U}$  which is positive semi-definite, we have

$$\ell(\alpha | \boldsymbol{\Lambda}) - \mathbb{E}[\varepsilon_q^2 | \boldsymbol{\Lambda}] = \sum_{i=1}^d v_{ii} \gamma_i (1 - \alpha \gamma_i)^{2T}.$$

where  $v_{ii} \geq 0$  for all  $i \in [d]$ . Without loss of generality, we assume that  $v_{ii}$  and  $\gamma_i$  are non-increasing in  $i \in [d]$ . Letting  $\gamma_{\max} = \gamma_1$  denote the largest eigenvalue of  $\boldsymbol{\Lambda}$ , we have that  $\gamma_{\max} = 1 + \|\mathbf{m}\|^2 = Z$  and  $\gamma_i = 1$  for  $i \geq 2$ . Since  $\mathbb{E}[\zeta^2] = 1$ , we have

$$\boldsymbol{\Sigma}_w = \frac{\mathbf{m} \mathbf{m}^\top}{(1 + \|\mathbf{m}\|^2)^2} = \frac{1}{Z} (\mathbf{I} - \boldsymbol{\Lambda}^{-1})$$

and so  $v_{11} = (Z - 1)/Z^2$  and  $v_{ii} = 0$  for  $i \geq 2$ . The conditional loss then simplifies to

$$\ell(\alpha|\mathbf{\Lambda}) = \frac{Z-1}{Z}(1-\alpha Z)^{2T} + \mathbb{E}[\varepsilon_q^2 | \mathbf{\Lambda}].$$

Moreover,

$$\mathbb{E}[\varepsilon_q^2 | \mathbf{\Lambda}] = \mathbb{E}\left[\frac{\zeta^2}{1 + \|\mathbf{m}\|^2} \mid \mathbf{\Lambda}\right] = \frac{1}{Z}.$$

Thus, up to the additive constant  $\mathbb{E}[1/Z]$ , the unconditional loss is given by

$$\ell(\alpha) = \mathbb{E}\left[\frac{Z-1}{Z}(1-\alpha Z)^{2T}\right]$$

as claimed.

1. Since  $\frac{Z-1}{Z}(1-\alpha Z)^{2T}$  is strictly convex in  $\alpha$  for  $Z > 0$  and  $\mathbb{P}(Z > 0) > 0$  by assumption 6.1, it follows that  $\ell(\alpha)$  is strictly convex. Similarly, coercivity of  $\frac{Z-1}{Z}(1-\alpha Z)^{2T}$  carries over to  $\ell(\alpha)$  by simply taking the expectation.
2. By (1),  $\ell(\alpha)$  has a unique minimizer. The first derivative of the loss is given by

$$\ell'(\alpha) = -2T\mathbb{E}[(Z-1)(1-\alpha Z)^{2T-1}].$$

Hence,

$$\text{sign}(\ell'(\alpha)) = \begin{cases} -1, & \text{if } \alpha \leq 0, \\ 1, & \text{if } \alpha \geq 1, \end{cases}$$

since  $(1-\alpha Z)^{2T-1} \leq 0$  when  $\alpha \geq 1$  because  $Z \geq 1$ . Thus, the unique root of  $\ell'(\alpha)$  is contained in  $(0, 1)$ . □

## D.1 Convergence of gradient flow

Given the above established properties of  $\ell(\alpha)$ , by standard dynamical systems theory results, we can derive the global convergence of gradient flow on the one-parameter loss. We include a detailed proof to initiate the unfamiliar reader.

**Lemma D.2** (One-parameter gradient flow convergence). *Suppose Assumption 6.1 holds. Then, gradient flow on  $\ell(\alpha)$  converges globally to the unique minimum of  $\ell$  whose existence is guaranteed by Lemma D.1.*

*Proof.* Let  $(\alpha_t)_{t \geq 0}$  be the gradient flow trajectory initialized at  $\alpha_0 \in \mathbb{R}$  and let  $\alpha^*$  denote the unique minimizer of  $\ell(\alpha)$ . By chain rule and the definition of gradient flow, we have

$$\frac{d}{dt}\ell(\alpha_t) = \nabla_{\alpha}\ell(\alpha_t)\dot{\alpha}_t = -\|\nabla_{\alpha}\ell(\alpha_t)\|^2 \leq 0.$$

Hence, the trajectory of the loss function  $\ell(\alpha_t)$  is decreasing and since  $\ell(\alpha) \geq 0$ , it follows that  $\ell(\alpha_t)$  converges as  $t \rightarrow \infty$ . Moreover, by coercivity of  $\ell$ ,  $\alpha_t \in \{\alpha : \ell(\alpha) \leq \ell(\alpha_0)\}$  for all  $t$  which is compact. Thus, as  $\ell \in C^\infty$ ,  $\ell'(\alpha_t)$  is uniformly continuous for all  $t \geq 0$ . Then, by Barbalat's Lemma [Slotine et al., 1991],  $\ell'(\alpha_t) \rightarrow 0$  as  $t \rightarrow \infty$ . As  $\alpha_t \in \{\alpha : \ell(\alpha) \leq \ell(\alpha_0)\}$  which is compact, moving to a convergent subsequence,  $\alpha_{t_k} \rightarrow \bar{\alpha}$  as  $k \rightarrow \infty$ . By continuity of  $\ell'$ ,  $\ell'(\alpha_{t_k}) \rightarrow \ell'(\bar{\alpha}) = 0$ . Hence,  $\bar{\alpha} = \alpha^*$  which is the unique minimizer of  $\ell$ . Hence, as every subsequence of  $(\alpha_t)_{t \geq 1}$  converges to  $\alpha^*$ , it follows that  $\alpha_t \rightarrow \alpha^*$  as  $t \rightarrow \infty$ . □

## D.2 Asymptotic depth behavior

Having thus far established the convergence of gradient flow at finite depth  $T$ , we now complete the proof of Theorem 6.2 with the following result which shows that as  $T \rightarrow \infty$ , we recover the optimal prediction of the model. Formally, let  $\alpha_T^*$  denote the limit of the gradient flow on the  $T$ -layer model which, from Lemma D.2, exists and coincides with the global minimum of  $\ell(\alpha)$ .

**Theorem D.3.** *Suppose Assumption 6.1 holds. Let  $\alpha_T^*$  denote the global minimum of  $\ell(\alpha)$  for the  $T$ -layer CA model which exists uniquely by Lemma D.1. Then,*

$$\lim_{T \rightarrow \infty} \alpha_T^* =: \alpha_\infty^* = \frac{2}{2 + \underline{m} + \overline{m}} = \frac{2}{\underline{Z} + \overline{Z}}.$$

Hence, the model is Bayes optimal by Lemmas C.1 and C.2.

*Proof.* Consider for  $\alpha \in [0, 1]$ , the function

$$\phi(\alpha) := \max_{z \in [\underline{Z}, \overline{Z}]} |1 - \alpha z| = \max\{|1 - \alpha \underline{Z}|, |1 - \alpha \overline{Z}|\}.$$

As the composition of a convex function with an affine function,  $z \mapsto |1 - \alpha z|$  is convex. On any interval, the maximum of a convex function occurs at the interval's endpoints and so

$$\phi(\alpha) = \max\{|1 - \alpha \underline{Z}|, |1 - \alpha \overline{Z}|\}.$$

Note that  $\phi(\alpha)$  is convex as the maximum of convex functions. The minimum of  $\phi(\alpha)$  occurs when  $|1 - \alpha \underline{Z}| = |1 - \alpha \overline{Z}|$ . Since  $\underline{Z} < \overline{Z}$ , the balancing occurs at opposite signs  $1 - \alpha \underline{Z} = -(1 - \alpha \overline{Z})$  which yields a unique minimizer

$$\alpha_\infty^* = \frac{2}{\underline{Z} + \overline{Z}}.$$

Now, let

$$f_T(\alpha) := \mathbb{E} \left[ \frac{Z-1}{Z} (1 - \alpha Z)^{2T} \right]^{1/2T}.$$

We use a shorthand  $W = \frac{Z-1}{Z}$  and  $X_\alpha = (1 - \alpha Z)$  so that

$$f_T(\alpha) = \mathbb{E}[W X_\alpha^{2T}]^{1/2T}.$$

Since  $X_\alpha \leq \phi(\alpha)$  and  $\mathbb{P}(W > 0) > 0$  by the assumption that  $\overline{Z} > \underline{Z} \geq 1$  (so  $\mathbb{E}[W] > 0$ ), we have

$$\limsup_{T \rightarrow \infty} f_T(\alpha) \leq \limsup_{T \rightarrow \infty} \mathbb{E}[W]^{1/2T} \phi(\alpha) = \phi(\alpha). \quad (\text{D.1})$$

Now, let  $(\alpha_T)_{T \geq 1}$  be a converging sequence with  $\alpha := \lim_{T \rightarrow \infty} \alpha_T$ . Notice that

$$\begin{aligned} \|X_{\alpha_T} - X_\alpha\|_\infty &= \||1 - \alpha_T Z| - |1 - \alpha Z|\|_\infty \\ &\leq \|(\alpha_T - \alpha)Z\|_\infty \\ &\leq |\alpha_T - \alpha| \overline{Z} \xrightarrow{T \rightarrow \infty} 0. \end{aligned}$$

Fixing  $\varepsilon \in (0, 1)$ , the above implies  $\|X_{\alpha_T} - X_\alpha\|_\infty \leq 1 - \varepsilon$  for  $T$  sufficiently large. The set  $S_\varepsilon := \{|X_\alpha| > \varepsilon \|X_\alpha\|_\infty\}$  satisfies  $\mathbb{P}(S_\varepsilon) > 0$  by definition of  $\|\cdot\|_\infty$ . Moreover, since  $W > 0$  a.s., there exists  $n \in \mathbb{N}$  such

that for  $A_n := \{W > 1/n\}$ , we have  $\mathbb{P}(A_n \cap S_\varepsilon) > 0$ . Putting things together, we have

$$\begin{aligned}
f_T(\alpha_T) &\geq \mathbb{E}[W X_{\alpha_T}^{2T} \mathbf{1}_{S_\varepsilon \cap A_n}]^{1/2T} \\
&\geq \left(\frac{1}{n}\right)^{1/2T} \mathbb{E}[ (|X_\alpha| - \|X_{\alpha_T} - X_\alpha\|_\infty)^{2T} \mathbf{1}_{S_\varepsilon \cap A_n} ]^{1/2T} \\
&\geq \left(\frac{1}{n}\right)^{1/2T} \mathbb{E}[(\varepsilon \|X_\alpha\|_\infty - \varepsilon + 1)^{2T} \mathbf{1}_{S_\varepsilon \cap A_n}]^{1/2T} \\
&= \left(\frac{\mathbb{P}(S_\varepsilon \cap A_n)}{n}\right)^{1/2T} (\varepsilon \|X_\alpha\|_\infty - \varepsilon + 1) \\
&\xrightarrow{T \rightarrow \infty} \varepsilon \|X_\alpha\|_\infty - \varepsilon + 1
\end{aligned}$$

Noticing that  $\phi(\alpha) = \|X_\alpha\|_\infty$ , taking  $\varepsilon \uparrow 1$ , we obtain

$$\liminf_{T \rightarrow \infty} f_T(\alpha_T) \geq \phi(\alpha). \quad (\text{D.2})$$

Now, note that  $(\alpha_T^*)_{T \geq 1} \subset [0, 1]$  by Lemma D.1(2). Therefore, we can extract a convergent subsequence  $(\alpha_{T_k}^*)_{k \geq 1}$  whose limit we denote by  $\bar{\alpha}$ . Since  $\alpha_{T_k}^*$  minimizes  $\ell$  (at depth  $T_k$ ) and hence  $f_{T_k}$ , from (D.1), we have

$$f_{T_k}(\alpha_{T_k}^*) \leq f_{T_k}(\alpha_\infty^*) \implies \limsup_{k \rightarrow \infty} f_{T_k}(\alpha_{T_k}^*) \leq \phi(\alpha_\infty^*).$$

Applying (D.2), we then have

$$\phi(\bar{\alpha}) \leq \liminf_{k \rightarrow \infty} f_{T_k}(\alpha_{T_k}^*) \leq \limsup_{k \rightarrow \infty} f_{T_k}(\alpha_{T_k}^*) \leq \phi(\alpha_\infty^*).$$

Since  $\alpha_\infty^*$  is the unique minimizer of  $\phi$ , it follows that  $\bar{\alpha} = \alpha_\infty^*$ . This completes the proof since if every convergent subsequence has the same limit, it follows that the sequence itself converges and shares this limit.  $\square$

## E Proof of Theorem 6.3

We now turn our attention to the model with the pair of learnable parameters  $(\alpha, \beta)$ . As before, we begin by determining a simplified form for the loss  $\ell(\alpha, \beta)$  and collect some properties. Recall,  $Z = 1 + \|\mathbf{m}\|^2$ .

Let

$$S := S(Z, \beta) = \frac{(1 + \beta Z)^T - 1}{\beta} \quad \text{where} \quad S(Z, 0) = \lim_{\beta \rightarrow 0} S(\beta, Z) = TZ,$$

$$W = \frac{Z - 1}{Z},$$

and

$$A(\beta) = \mathbb{E}[W S^2], \quad B(\beta) = \mathbb{E}[W S].$$

**Lemma E.1** (Two-parameter loss). *The loss  $\ell(\alpha, \beta)$  has the form*

$$\ell(\alpha, \beta) = \mathbb{E} \left[ \frac{Z - 1}{Z} \left( \frac{\alpha}{\beta} [(1 + \beta Z)^T - 1] - 1 \right)^2 \right]$$

up to the additive constant  $\mathbb{E}[1/Z]$ . Moreover, for fixed  $\beta \in \mathbb{R}$ , the loss is strongly convex in  $\alpha$ , with unique minimizer:

$$\alpha^*(\beta) := \frac{B(\beta)}{A(\beta)}.$$

*Proof.* We have

$$\begin{aligned}
\frac{\mathbf{y}^\top \mathbf{F}^\top \mathbf{x}_q}{L} &= \frac{\mathbf{w}^\top \mathbf{X} \mathbf{F}^\top \mathbf{x}_q}{L} + \frac{\boldsymbol{\varepsilon}^\top \mathbf{F}^\top \mathbf{x}_q}{L} \\
&= \frac{\alpha}{\beta} \mathbf{w}^\top (\mathbf{M}^T - \mathbf{I}) \mathbf{x}_q + \frac{\boldsymbol{\varepsilon}^\top \mathbf{F}^\top \mathbf{x}_q}{L} \\
&= -\frac{\alpha}{\beta} \mathbf{w}^\top \mathbf{x}_q + \frac{\alpha}{\beta} \mathbf{w}^\top (\mathbf{I} + \beta \hat{\boldsymbol{\Lambda}})^T \mathbf{x}_q + \frac{\boldsymbol{\varepsilon}^\top \mathbf{F}^\top \mathbf{x}_q}{L}.
\end{aligned}$$

and so

$$y_q - \hat{y}_q = \left(1 + \frac{\alpha}{\beta}\right) \mathbf{w}^\top \mathbf{x}_q - \frac{\alpha}{\beta} \mathbf{w}^\top (\mathbf{I} + \beta \hat{\boldsymbol{\Lambda}})^T \mathbf{x}_q - \frac{\boldsymbol{\varepsilon}^\top \mathbf{F}^\top \mathbf{x}_q}{L} + \varepsilon_q.$$

Taking  $L \rightarrow \infty$  so that  $\frac{\boldsymbol{\varepsilon}^\top \mathbf{F}^\top \mathbf{x}_q}{L}$  is negligible, and omitting  $\mathbb{E}[\varepsilon_q^2 | \boldsymbol{\Lambda}]$  which does not depend on  $(\alpha, \beta)$ , we have, up to the additive constant  $\mathbb{E}[1/Z]$ ,

$$\begin{aligned}
\ell(\alpha, \beta | \boldsymbol{\Lambda}) &\propto \left(1 + \frac{\alpha}{\beta}\right)^2 \mathbb{E}[(\mathbf{w}^\top \mathbf{x}_q)^2 | \boldsymbol{\Lambda}] + \left(\frac{\alpha}{\beta}\right)^2 \mathbb{E}[(\mathbf{w}^\top (\mathbf{I} + \beta \boldsymbol{\Lambda})^T \mathbf{x}_q)^2 | \boldsymbol{\Lambda}] \\
&\quad - \frac{2\alpha}{\beta} \left(1 + \frac{\alpha}{\beta}\right) \mathbb{E}[\mathbf{w}^\top \mathbf{x}_q \mathbf{w}^\top (\mathbf{I} + \beta \boldsymbol{\Lambda})^T \mathbf{x}_q | \boldsymbol{\Lambda}] \\
&= \left(1 + \frac{\alpha}{\beta}\right)^2 \text{tr}(\boldsymbol{\Sigma}_w \boldsymbol{\Lambda}) + \left(\frac{\alpha}{\beta}\right)^2 \text{tr}(\boldsymbol{\Sigma}_w \boldsymbol{\Lambda} (\mathbf{I} + \beta \boldsymbol{\Lambda})^{2T}) \\
&\quad - \frac{2\alpha}{\beta} \left(1 + \frac{\alpha}{\beta}\right) \text{tr}(\boldsymbol{\Sigma}_w \boldsymbol{\Lambda} (\mathbf{I} + \beta \boldsymbol{\Lambda})^T).
\end{aligned}$$

In the first line we used that  $\mathbb{E}[\varepsilon_i] = 0$  to get rid of cross terms and in the second, we use that  $\boldsymbol{\Sigma}_w$  commutes with  $\boldsymbol{\Lambda}$ . Recalling that

$$\boldsymbol{\Sigma}_w = \frac{\mathbf{m} \mathbf{m}^\top}{(1 + \|\mathbf{m}\|^2)^2} = \frac{1}{Z} (\mathbf{I} - \boldsymbol{\Lambda}^{-1}),$$

the loss simplifies to

$$\begin{aligned}
\ell(\alpha, \beta | \boldsymbol{\Lambda}) &= \left(1 + \frac{\alpha}{\beta}\right)^2 \frac{1}{Z} \sum_{i=1}^d (\gamma_i - 1) + \left(\frac{\alpha}{\beta}\right)^2 \frac{1}{Z} \sum_{i=1}^d (\gamma_i - 1) (1 + \beta \gamma_i)^{2T} \\
&\quad - 2 \frac{\alpha}{\beta} \left(1 + \frac{\alpha}{\beta}\right) \frac{1}{Z} \sum_{i=1}^d (\gamma_i - 1) (1 + \beta \gamma_i)^T \\
&= \left(1 + \frac{\alpha}{\beta}\right)^2 \frac{Z-1}{Z} + \left(\frac{\alpha}{\beta}\right)^2 \frac{Z-1}{Z} (1 + \beta Z)^{2T} \\
&\quad - 2 \frac{\alpha}{\beta} \left(1 + \frac{\alpha}{\beta}\right) \frac{Z-1}{Z} (1 + \beta Z)^T \\
&= \frac{Z-1}{Z} \left(\frac{\alpha}{\beta} [(1 + \beta Z)^T - 1] - 1\right)^2.
\end{aligned}$$

For the unconditional loss, one simply takes expectation:

$$\ell(\alpha, \beta) = \mathbb{E} \left[ \frac{Z-1}{Z} \left(\frac{\alpha}{\beta} [(1 + \beta Z)^T - 1] - 1\right)^2 \right].$$

Expanding the above square, we see

$$\ell(\alpha, \beta) = \alpha^2 \mathbb{E}[W S^2] - 2\alpha \mathbb{E}[W S] + \mathbb{E}[W] = \alpha^2 A(\beta) - 2\alpha B(\beta) + \mathbb{E}[W]$$

is quadratic in  $\alpha$ —hence strongly convex—and thus has a unique minimizer at  $B(\beta)/A(\beta)$ .  $\square$

In light of Lemma E.1, profiling out  $\alpha$ , we can write a reduced loss

$$F_T(\beta) := \min_{\alpha \in \mathbb{R}} \ell(\alpha, \beta) = \ell(\alpha^*(\beta), \beta) = \mathbb{E}[W] - \frac{B(\beta)^2}{A(\beta)}.$$

At this point, we notice that neither the loss  $\ell(\alpha, \beta)$  nor the reduced loss  $F_T(\beta)$  are convex. Hence, the subsequent analysis establishing the convergence of gradient flow will require a different and more involved route than in the one-parameter setup.

## E.1 Convergence of gradient flow

In this section, we establish that at finite depth  $T$ , gradient flow on the two-parameter loss converges under suitable initialization. We first show that, regardless of initialization, the iterates  $(\alpha_t)_{t \geq 0}$  remain bounded. Then, we show that the iterates  $(\beta_t)_{t \geq 0}$  remain bounded if one initializes  $\beta_0 \in (-2/\bar{Z}, 0)$  and  $\alpha_0 = \alpha^*(\beta_0)$ . Under this setup where the iterates  $(\alpha_t, \beta_t)_{t \geq 0}$  remain bounded, we conclude by showing they must converge as  $t \rightarrow \infty$ , hence establishing convergence of the gradient flow procedure at finite layer-depth.

We first establish some preliminary properties of the function  $A(\beta)$ .

**Lemma E.2.** *Suppose Assumption 6.1 holds. Then,*

1.  $A(\beta)$  is continuous and  $\lim_{|\beta| \rightarrow \infty} A(\beta) = +\infty$ .
2.  $A^* := \inf_{\beta \in \mathbb{R}} A(\beta) > 0$ .

*Proof.* 1. Continuity follows readily by the dominated convergence theorem which may be applied as  $Z \in [\underline{Z}, \bar{Z}]$  almost surely. Let  $z_0 \in (1, \bar{Z}]$  be such that  $\mathbb{P}(Z \geq z_0) > 0$ . Then, as  $|\beta| \rightarrow \infty$ , we have

$$S(\beta, z)^2 = \left( z \sum_{k=0}^{T-1} (1 + \beta z)^k \right)^2 \asymp z^2 (1 + \beta z)^{2T-2}$$

and so  $S(\beta, z)^2 \geq z_0^2 (1 + \beta z_0)^{2T-2}$  for  $z \geq z_0$ . Thus,

$$A(\beta) = \mathbb{E}[WS^2] \geq \mathbb{E}[W \mathbf{1}_{Z \geq z_0}] z_0^2 (1 + \beta z_0)^{2T-2} \xrightarrow{|\beta| \rightarrow \infty} \infty.$$

2. Let  $C > 0$ , then on the compact set  $[-C, C]$ , by continuity of  $A(\beta)$ , its minimum  $A_{\min} := \min_{|\beta| \leq C} A(\beta)$  is attained. Assume for contradiction that  $A_{\min} = 0$ . Then,  $S(\beta^*, Z) = 0$  almost surely on  $\{Z > 1\}$  for some  $\beta^*$ . Since  $Z$  has a continuous non-degenerate distribution, this implies that

$$\sum_{k=0}^{T-1} (1 + \beta^* z)^k = 0$$

for uncountably many values of  $z$ , which is impossible for a non-zero polynomial. Hence  $A_{\min} > 0$ . As  $\lim_{|\beta| \rightarrow \infty} A(\beta) = +\infty$ , it follows that  $A^* := \inf_{\beta \in \mathbb{R}} A(\beta) > 0$ . □

We can show that the iterates  $(\alpha_t)_{t \geq 0}$  remain bounded regardless of initialization.

**Lemma E.3.** *Suppose Assumption 6.1 holds. Then,*

$$\sup_{\beta \in \mathbb{R}} |\alpha^*(\beta)| \leq \sqrt{\frac{\mathbb{E}[W]}{A^*}} =: M^* < \infty.$$

Moreover, letting  $(\alpha_t, \beta_t)_{t \geq 0}$  be any gradient flow trajectory on  $\ell$ , we have

$$\sup_{t \geq 0} |\alpha_t| \leq M^* + \sqrt{\frac{\ell(\alpha_0, \beta_0)}{A^*}} =: M_{\alpha_0, \beta_0} < \infty.$$

*Proof.* By the Cauchy-Schwarz inequality,

$$B(\beta)^2 = \mathbb{E}[W^{1/2} \cdot W^{1/2} S(\beta)]^2 \leq \mathbb{E}[W] \mathbb{E}[W S(\beta)^2] = \mathbb{E}[W] A(\beta).$$

By Lemma E.2,

$$\sup_{\beta \in \mathbb{R}} |\alpha^*(\beta)| = \sup_{\beta \in \mathbb{R}} \frac{|B(\beta)|}{A(\beta)} \leq \sqrt{\frac{\mathbb{E}[W]}{A^*}} = M^* < \infty.$$

Now, setting  $\Delta_t = \alpha_t - \alpha^*(\beta_t)$ , notice that we may write

$$\ell(\alpha, \beta) = A(\beta) \Delta^2 + \underbrace{\mathbb{E}[W] - \frac{B(\beta)^2}{A(\beta)}}_{:=C(\beta) \geq 0}$$

where the non-negativity of  $C(\beta)$  follows from the inequality  $B(\beta)^2 \leq \mathbb{E}[W] A(\beta)$ . Recall that the loss  $\ell$  is non-increasing along gradient flow for all  $t \geq 0$  which follows from  $\frac{d}{dt} \ell(\alpha_t, \beta_t) = -\|\nabla \ell(\alpha_t, \beta_t)\|^2 \leq 0$ . Hence,  $\ell(\alpha_t, \beta_t) \leq \ell(\alpha_0, \beta_0)$  for all  $t \geq 0$  and so

$$A(\beta_t) \Delta_t^2 = \ell(\alpha_t, \beta_t) - C(\beta_t) \leq \ell(\alpha_0, \beta_0).$$

Since  $A(\beta_t) \geq A^*$  by Lemma E.2, we obtain  $\sup_{t \geq 0} |\Delta_t| \leq \sqrt{\ell(\alpha_0, \beta_0)/A^*}$  and so

$$\sup_{t \geq 0} |\alpha_t| \leq \sup_{t \geq 0} |\alpha^*(\beta_t)| + \sup_{t \geq 0} |\Delta_t| \leq M^* + \sqrt{\frac{\ell(\alpha_0, \beta_0)}{A^*}} < \infty$$

as desired.  $\square$

Now, focusing on the iterates  $(\beta_t)_{t \geq 0}$ , the following result shows that these iterates remain bounded. It is convenient to introduce the probability measure

$$d\mu = \frac{W}{\mathbb{E}[W]} d\mathbb{P}$$

so that  $\mu$  is obtained by reweighting  $d\mathbb{P}$  by  $W$  and  $\mathbb{E}_\mu[Y] = \mathbb{E}[WY]/\mathbb{E}[W]$  for a random variable  $Y$ . The following remark contains a technical device which is generic under Assumption 6.1.

*Remark E.4* (Density of  $Z$  under  $\mu$ ). Suppose that under  $\mu$ ,  $Z$  has density  $g$  with respect to the Lebesgue measure on  $[\underline{Z}, \bar{Z}]$  such that (i)  $g$  is continuous; (ii)  $g(\underline{Z}) > 0$ ; and (iii)  $g(\bar{Z}) > 0$ .

Writing

$$u_T(\beta, Z) := (1 + \beta Z)^T,$$

a short calculation shows

$$F_T(\beta) = \mathbb{E}[W] \frac{\text{Var}_\mu(u_T(\beta, Z))}{\mathbb{E}_\mu[(1 - u_T(\beta, Z))^2]} \quad (\text{E.1})$$

for any  $\beta \neq 0$  which will provide a convenient representation of the loss in subsequent proofs.

**Lemma E.5.** *Suppose Assumption 6.1 holds and the conditions of Remark E.4 are satisfied, and that one initializes gradient flow at  $\alpha_0 = \alpha^*(\beta_0)$  with  $\beta_0 \in (-2/\bar{Z}, 0)$ . Then, there exists  $T' = T'(\beta_0) \in \mathbb{N}$  such that for all  $T \geq T'$ , we have*

$$\ell(\alpha_0, \beta_0) < \min\{\ell(\alpha, -2/\bar{Z}), \ell(\alpha, 0)\}$$

for all  $\alpha \in \mathbb{R}$ . Consequently, since gradient flow is non-increasing on the loss  $\ell$ , one has  $(\beta_t)_{t \geq 0} \subset (-2/\bar{Z}, 0)$ .

*Proof.* For  $\beta = 0$ , a quick derivation reveals

$$\ell(\alpha, 0) \geq \ell(\alpha^*(0), 0) = \mathbb{E}[W] - \frac{(\mathbb{E}[WZ])^2}{\mathbb{E}[WZ^2]} =: c > 0$$

for all  $\alpha \in \mathbb{R}$  by Cauchy-Schwarz where  $c$  does not depend on  $T$ . At  $\beta = -2/\bar{Z}$ , write

$$v_T(Z) := u_T(-2/\bar{Z}, Z) = (1 - 2Z/\bar{Z})^T.$$

Since  $|v_T(Z)| \leq 1$ , we have  $\mathbb{E}_\mu[(1 - u_T(\beta, Z))^2] \leq 4$ , and hence from (E.1),

$$\ell(\alpha, -2/\bar{Z}) \geq F_T(-2/\bar{Z}) \geq \frac{\mathbb{E}[W]}{4} \text{Var}_\mu(v_T(Z))$$

for all  $\alpha \in \mathbb{R}$ . We now show that  $\text{Var}_\mu(v_T(Z)) = \Omega(1/T)$ . From Remark E.4, let  $g$  denote the continuous density of  $\mu$  on  $[\underline{Z}, \bar{Z}]$ , so that  $\mathbb{E}_\mu[h(Z)] = \int_{\underline{Z}}^{\bar{Z}} h(z)g(z) dz$  and in particular, there exist  $\delta > 0$  and  $c_1 > 0$  such that

$$g(z) \geq c_1 \quad \text{for all } z \in [\bar{Z} - \delta, \bar{Z}]. \quad (\text{E.2})$$

By a change of variables  $z = \bar{Z} - y$  for  $y \in [0, \bar{Z} - \underline{Z}]$  and taking  $T$  sufficiently large so that  $1/T \leq \delta$ , we have

$$\begin{aligned} \mathbb{E}_\mu[v_T(Z)^2] &= \int_{\underline{Z}}^{\bar{Z}} (1 - 2z/\bar{Z})^{2T} g(z) dz = \int_0^{\bar{Z} - \underline{Z}} (1 - 2y/\bar{Z})^{2T} g(\bar{Z} - y) dy \\ &\geq \int_0^{1/T} (1 - 2y/\bar{Z})^{2T} g(\bar{Z} - y) dy \geq c_1 \int_0^{1/T} (1 - 2y/\bar{Z})^{2T} dy. \end{aligned}$$

where we used (E.2) for the last inequality. For  $T$  sufficiently large and  $y \in [0, 1/T]$ , we have  $2y/\bar{Z} \leq 1/2$  and so applying the standard inequality  $1 - x \geq e^{-2x}$  for  $x \in [0, 1/2]$  yields

$$\mathbb{E}_\mu[v_T(Z)^2] \geq c_1 \int_0^{1/T} \exp\left(-\frac{8Ty}{\bar{Z}}\right) dy \geq c_1 \int_0^{1/T} \exp\left(-\frac{8}{\bar{Z}}\right) dy = \Omega(1/T).$$

We now turn our attention to  $\mathbb{E}_\mu[v_T(Z)]^2$ . Since  $g$  is continuous on  $[\underline{Z}, \bar{Z}]$ , let  $c_2$  be an upper bound on  $g$  and assume without loss of generality that  $\bar{Z}/2 \leq \bar{Z} - \underline{Z}$ <sup>3</sup>. Using the inequality  $1 - x \leq e^{-x}$  for  $x \in [0, 1]$  and  $|1 - 2y/\bar{Z}| =: \bar{\rho} < 1$  for all  $y \in [\bar{Z}/2, \bar{Z} - \underline{Z}]$ , we have

$$\begin{aligned} \mathbb{E}_\mu[|v_T(Z)|] &= \int_{\underline{Z}}^{\bar{Z}} |1 - 2z/\bar{Z}|^T g(z) dz = \int_0^{\bar{Z} - \underline{Z}} |1 - 2y/\bar{Z}|^T g(\bar{Z} - y) dy \\ &\leq c_2 \int_0^{\bar{Z}/2} |1 - 2y/\bar{Z}|^T dy + c_2 \int_{\bar{Z}/2}^{\bar{Z} - \underline{Z}} |1 - 2y/\bar{Z}|^T dy \\ &\leq c_2 \int_0^{\bar{Z}/2} \exp(-2Ty/\bar{Z}) dy + c_2 \int_{\bar{Z}/2}^{\bar{Z} - \underline{Z}} \bar{\rho}^T dy \\ &\leq c_2 \left( \int_0^\infty \exp(-2Ty/\bar{Z}) dy + (\bar{Z} - \underline{Z})\bar{\rho}^T \right) \\ &\leq c_2 \left( \frac{\bar{Z}}{2T} + (\bar{Z} - \underline{Z})\bar{\rho}^T \right) = O(1/T). \end{aligned}$$

By Jensen's inequality, we have  $\mathbb{E}_\mu[v_T(Z)]^2 = O(1/T^2)$  and so  $\text{Var}_\mu(v_T(Z)) = \Omega(1/T)$ . Hence, for all  $\alpha \in \mathbb{R}$ ,

$$\ell(\alpha, -2/\bar{Z}) = \Omega(1/T) \quad (\text{E.3})$$

<sup>3</sup>If this is not the case, the analysis below is simplified.

for all  $T$  large. Finally, note that for the fixed initialization  $\beta_0 \in (-2/\bar{Z}, 0)$ , we have

$$|u_T(\beta_0, Z)| \leq \rho_{\beta_0}^T \quad \text{for some } \rho_{\beta_0} \in (0, 1)$$

almost surely. Hence, there exists  $\bar{T}$  such that  $\mathbb{E}_\mu[(1 - u_T(\beta_0, Z))^2] \geq C > 0$  (e.g.  $C = 1/2$ ) for all  $T \geq \bar{T}$ , and so

$$F_T(\beta_0) \leq \frac{\mathbb{E}[W]\text{Var}_\mu(u_T(\beta_0, Z))}{C} \leq \frac{\mathbb{E}[W]\mathbb{E}_\mu[u_T(\beta_0, Z)^2]}{C} \leq \frac{\mathbb{E}[W]}{C}\rho_{\beta_0}^{2T} = O(\rho_{\beta_0}^{2T}).$$

Since  $\alpha_0 = \alpha^*(\beta_0)$ , we have

$$\ell(\alpha_0, \beta_0) = F_T(\beta_0) = O(\rho_{\beta_0}^{2T}).$$

Combining this with (E.3) and the lower bound  $\ell(\alpha, 0) \geq c > 0$ , it follows that there exists  $T' = T'(\beta_0)$  such that for all  $T \geq T'$ ,

$$\ell(\alpha_0, \beta_0) < \min\{\ell(\alpha, -2/\bar{Z}), \ell(\alpha, 0)\} \quad \forall \alpha \in \mathbb{R}.$$

The final claim follows because gradient flow is non-increasing on  $\ell$ .  $\square$

**Theorem E.6.** *Suppose Assumption 6.1 holds and the conditions of Remark E.4 are satisfied, and that one initializes gradient flow at  $\alpha_0 = \alpha^*(\beta_0)$  with  $\beta_0 \in (-2/\bar{Z}, 0)$ . Then, gradient flow on  $\ell(\alpha, \beta)$  converges with*

$$\beta_T^* := \lim_{t \rightarrow \infty} \beta_{t,T} \in (-2/\bar{Z}, 0)$$

and

$$\alpha_T^* := \lim_{t \rightarrow \infty} \alpha_{t,T} = \alpha^*(\beta_T^*).$$

*Proof.* By Lemma E.5, since gradient flow is non-increasing on  $\ell(\alpha, \beta)$ , it follows that  $\beta_t \in (-2/\bar{Z}, 0)$  for all  $t \geq 0$ . Moreover, from Lemma E.3, we know that  $\alpha_t$  remains bounded and so the gradient flow trajectory  $(\alpha_t, \beta_t)_{t \geq 0}$  is bounded. Since  $\ell$  is real-analytic on the open set  $\mathbb{R} \times (-2/\bar{Z}, 0)$ , the bounded trajectory  $(\alpha_t, \beta_t)_{t \geq 0}$  converges to a single critical point by the Lojasiewicz gradient inequality. Clearly,  $\alpha_T^* = \alpha^*(\beta_T^*)$  and since  $\beta_t \in (-2/\bar{Z}, 0)$  for all  $t \geq 0$ , it follows that  $\beta_T^* \in [-2/\bar{Z}, 0]$ . Moreover, by continuity of the loss  $\ell$  in  $(\alpha, \beta)$  and Lemma E.5 which shows  $\ell(\alpha_0, \beta_0) < \min\{\ell(\alpha, -2/\bar{Z}), \ell(\alpha, 0)\}$ ,  $\beta_T^* \notin \{-2/\bar{Z}, 0\}$  as if this were the case then necessarily, for  $t$  sufficiently large one would have  $\ell(\alpha_t, \beta_t) > \ell(\alpha_0, \beta_0)$ —a contradiction. Hence,  $\beta_T^*$  lies in the open interval  $(-2/\bar{Z}, 0)$ .  $\square$

## E.2 Asymptotic depth behavior

Having established in the previous subsection that gradient flow converges to a stationary point at any fixed depth  $T$ , we now study how these stationary points behave as the depth  $T \rightarrow \infty$ . Our goal is to understand the asymptotic depth behavior of the limits of gradient flow and to show that, as in the one-parameter case, the limiting predictor is Bayes optimal. To make explicit the dependence on depth, let  $\ell^{(T)}$  denote the loss  $\ell$  where the CA model is at depth  $T$ .

In the two-parameter setting, the loss is not jointly convex, so we cannot identify the gradient-flow limit  $(\alpha_T^*, \beta_T^*)$  as a global minimizer of  $\ell$ . However, what is guaranteed is that

$$(\alpha_T^*, \beta_T^*) \text{ is a stationary point of } \ell^{(T)} \quad \text{and} \quad \alpha_T^* = \alpha^*(\beta_T^*),$$

so in particular

$$F_T'(\beta_T^*) = 0.$$

Thus, the large-depth behavior of the gradient-flow limits is governed by the stationary points of the one-dimensional function  $\beta \mapsto F_T(\beta)$ . It will be convenient to work with a logarithmically rescaled version of  $F_T$ :

$$G_T(\beta) := \frac{1}{2T} \log \left( \frac{F_T(\beta)}{\mathbb{E}[W]} \right).$$

The function  $G_T$  is well-defined and smooth as  $F_T > 0$ . Moreover,  $G_T$  is a strictly monotone transform of  $F_T$  so  $F'_T(\beta_T^*) = 0$  if and only if  $G'_T(\beta_T^*) = 0$ . Our task is therefore to understand the asymptotic behavior of  $G_T$  and  $G'_T$  as  $T \rightarrow \infty$ , and to show that stationary points of  $F_T$  (and  $G_T$ ) concentrate near a single value of  $\beta$ .

**Lemma E.7.** *Suppose Assumption 6.1 holds and the conditions of Remark E.4 are satisfied, and fix any compact interval  $K \subset I \setminus \{-\alpha^*\}$ , where  $I := (-2/\bar{Z}, 0)$ ,  $\alpha^* := 2/(\underline{Z} + \bar{Z})$ . For each  $T \in \mathbb{N}$  and  $\beta \in K$  define the probability measure*

$$d\nu_{T,\beta}(z) := \frac{|1 + \beta z|^{2T}}{\int |1 + \beta s|^{2T} d\mu(s)} d\mu(z).$$

Then the following hold uniformly for  $\beta \in K$  as  $T \rightarrow \infty$ :

1. The reduced loss  $F_T(\beta)$  satisfies

$$F_T(\beta)^{1/(2T)} \longrightarrow \phi(\beta),$$

where

$$\phi(\beta) = \max\{|1 + \beta \underline{Z}|, |1 + \beta \bar{Z}|\}.$$

2. Let  $z^*(\beta) \in \{\underline{Z}, \bar{Z}\}$  denote the unique endpoint at which  $\phi(\beta) = |1 + \beta z^*(\beta)|$  is attained. Then  $\nu_{T,\beta}$  converges weakly to the point mass at the active endpoint.

*Proof.* We begin from the variance representation:

$$F_T(\beta) = \mathbb{E}[W] \frac{\text{Var}_\mu(u_T(\beta, Z))}{\mathbb{E}_\mu[(1 - u_T(\beta, Z))^2]}.$$

We analyze numerator and denominator separately. For the denominator, for any  $\beta \in K$  and  $z \in [\underline{Z}, \bar{Z}]$  we have

$$|1 + \beta z| \leq \phi(\beta) \leq \phi_K := \sup_{\beta \in K} \phi(\beta) < 1,$$

where  $\phi_K < 1$  by continuity of  $\phi$  and compactness of  $K$ . Thus,

$$|u_T(\beta, Z)| = |1 + \beta Z|^T \leq \phi_K^T$$

almost surely and therefore

$$\mathbb{E}_\mu[(1 - u_T(\beta, Z))^2] = 1 - 2\mathbb{E}_\mu[u_T(\beta, Z)] + \mathbb{E}_\mu[u_T(\beta, Z)^2],$$

with

$$|\mathbb{E}_\mu[u_T(\beta, Z)]| \leq \phi_K^T, \quad \mathbb{E}_\mu[u_T(\beta, Z)^2] \leq \phi_K^{2T}.$$

Hence

$$\mathbb{E}_\mu[(1 - u_T(\beta, Z))^2] \in [1 - 2\phi_K^T, 1 + \phi_K^{2T}] \xrightarrow{T \rightarrow \infty} 1$$

uniformly in  $\beta \in K$ . In particular, for all sufficiently large  $T$ , we have

$$\frac{1}{2} \leq \mathbb{E}_\mu[(1 - u_T(\beta, Z))^2] \leq 2, \quad \forall \beta \in K. \tag{E.4}$$

Now, for an upper bound on the numerator, we have

$$\text{Var}_\mu(u_T(\beta, Z)) \leq \mathbb{E}_\mu[u_T(\beta, Z)^2] = \int |1 + \beta z|^{2T} d\mu(z) \leq \phi(\beta)^{2T}. \quad (\text{E.5})$$

Now, for a lower bound on the numerator, note that for any random variable  $X$  and measurable event  $A$ , the law of total variance shows:

$$\text{Var}_\mu(X) \geq \mu(A)\mu(A^c) (\mathbb{E}[X | A] - \mathbb{E}[X | A^c])^2. \quad (\text{E.6})$$

Now, for fixed  $\beta \in K$ , we define

$$X_T(\beta) := u_T(\beta, Z) = (1 + \beta Z)^T.$$

Since the conditions of Remark E.4 hold and  $K$  is compact, there exist constants  $\varepsilon > 0$  and  $c > 0$  such that, for every  $\beta \in K$ ,

- if  $z^*(\beta) = \bar{Z}$ , then  $A_\beta := [\bar{Z} - \varepsilon, \bar{Z}]$  satisfies  $\mu(A_\beta) \geq c$ ;
- if  $z^*(\beta) = \underline{Z}$ , then  $A_\beta := [\underline{Z}, \underline{Z} + \varepsilon]$  satisfies  $\mu(A_\beta) \geq c$ .

Without loss of generality, by continuity of the map  $(\beta, z) \mapsto |1 + \beta z|$  on the compact set  $K \times [\underline{Z}, \bar{Z}]$ , we may also choose  $\varepsilon$  small enough so that there exists  $\delta \in (0, 1 - \phi_K)$  and  $\eta > 0$  with

$$|1 + \beta z| \geq \phi(\beta) - \delta \quad \text{for all } z \in A_\beta, \beta \in K, \quad (\text{E.7})$$

$$|1 + \beta z| \leq \phi(\beta) - \eta \quad \text{for all } z \in A_\beta^c, \beta \in K. \quad (\text{E.8})$$

Moreover, shrinking  $\varepsilon$  if necessary, we may assume that there exists  $\sigma \in \{-1, 1\}$  such that

$$\sigma(1 + \beta z) \geq 0 \quad \text{for all } z \in A_\beta, \beta \in K. \quad (\text{E.9})$$

Indeed, since  $K \subset I \setminus \{-\alpha^*\}$ , the active endpoint is unique for every  $\beta \in K$ , and by compactness of  $K$  the distance from  $K$  to  $-\alpha^*$  is strictly positive; this gives a uniform gap from zero for  $1 + \beta z$  on the corresponding endpoint neighborhood  $A_\beta$ .

From (E.7)–(E.8), we have  $|X_T(\beta)| \geq (\phi(\beta) - \delta)^T$  on  $A_\beta$  while  $|X_T(\beta)| \leq (\phi(\beta) - \eta)^T$  on  $A_\beta^c$ . By (E.9),  $X_T(\beta)$  has constant sign on  $A_\beta$ , and therefore

$$|\mathbb{E}[X_T(\beta) | A_\beta]| = \mathbb{E}[|X_T(\beta)| | A_\beta] \geq (\phi(\beta) - \delta)^T.$$

Also,

$$|\mathbb{E}[X_T(\beta) | A_\beta^c]| \leq (\phi(\beta) - \eta)^T.$$

Further, for all sufficiently large  $T$  we have  $(\phi(\beta) - \eta)^T \leq \frac{1}{2}(\phi(\beta) - \delta)^T$ , and so

$$|\mathbb{E}[X_T(\beta) | A_\beta] - \mathbb{E}[X_T(\beta) | A_\beta^c]| \geq (\phi(\beta) - \delta)^T - (\phi(\beta) - \eta)^T \geq \frac{1}{2}(\phi(\beta) - \delta)^T.$$

Applying the inequality (E.6) with  $X = X_T(\beta)$  and  $A = A_\beta$ , we obtain

$$\text{Var}_\mu(u_T(\beta, Z)) \geq \mu(A_\beta)\mu(A_\beta^c) (\mathbb{E}[X_T(\beta) | A_\beta] - \mathbb{E}[X_T(\beta) | A_\beta^c])^2 \geq C_1(\phi(\beta) - \delta)^{2T},$$

for all  $\beta \in K$  and all sufficiently large  $T$ , where  $C_1 := \frac{1}{4}c(1 - c) > 0$  is independent of  $\beta$ . Combining this with the upper bound (E.5), we have, for all large  $T$  and all  $\beta \in K$ ,

$$C_1(\phi(\beta) - \delta)^{2T} \leq \text{Var}_\mu(u_T(\beta, Z)) \leq \phi(\beta)^{2T}. \quad (\text{E.10})$$

Putting everything together, using (E.4) and (E.10), we obtain

$$\frac{1}{2}\mathbb{E}[W]\text{Var}_\mu(u_T(\beta, Z)) \leq F_T(\beta) \leq 2\mathbb{E}[W]\text{Var}_\mu(u_T(\beta, Z))$$

for all large  $T$  and all  $\beta \in K$ . Hence, for such  $T$ ,

$$\left(\frac{1}{2}\mathbb{E}[W]C_1\right)^{1/(2T)}(\phi(\beta) - \delta) \leq F_T(\beta)^{1/(2T)} \leq (2\mathbb{E}[W])^{1/(2T)}\phi(\beta).$$

Letting  $T \rightarrow \infty$ , we have

$$\phi(\beta) - \delta \leq \liminf_{T \rightarrow \infty} F_T(\beta)^{1/(2T)} \leq \limsup_{T \rightarrow \infty} F_T(\beta)^{1/(2T)} \leq \phi(\beta)$$

and, since  $\delta > 0$  was arbitrary, we obtain the desired uniform convergence over  $K$ .

We now turn to proving the second statement of the lemma. Fix a bounded, continuous function  $f : [\underline{Z}, \bar{Z}] \rightarrow \mathbb{R}$ . By definition of  $\nu_{T,\beta}$ ,

$$\int f(z) d\nu_{T,\beta}(z) = \frac{\int f(z) |1 + \beta z|^{2T} d\mu(z)}{\int |1 + \beta s|^{2T} d\mu(s)}. \quad (\text{E.11})$$

We will show that the right-hand side of (E.11) converges to  $f(z^*(\beta))$  uniformly in  $\beta \in K$ . Split both the numerator and denominator into contributions from  $A_\beta$  and  $A_\beta^c$ . From (E.7)–(E.8) we have

$$\int_{A_\beta} |1 + \beta z|^{2T} d\mu(z) \geq \mu(A_\beta)(\phi(\beta) - \delta)^{2T} \geq c(\phi(\beta) - \delta)^{2T}$$

and

$$\int_{A_\beta^c} |1 + \beta z|^{2T} d\mu(z) \leq (\phi(\beta) - \eta)^{2T}.$$

Thus,

$$\frac{\int_{A_\beta^c} |1 + \beta z|^{2T} d\mu(z)}{\int_{A_\beta} |1 + \beta z|^{2T} d\mu(z)} \leq \frac{(\phi(\beta) - \eta)^{2T}}{c(\phi(\beta) - \delta)^{2T}} \xrightarrow{T \rightarrow \infty} 0,$$

uniformly over  $\beta \in K$ . Therefore, the contribution of  $A_\beta^c$  to both the numerator and denominator in (E.11) is negligible. More precisely, write the numerator  $N_T(\beta)$  and denominator  $D_T(\beta)$  as

$$N_T(\beta) = \int f(z) |1 + \beta z|^{2T} d\mu(z) = N_T^{(A)}(\beta) + N_T^{(A^c)}(\beta),$$

$$D_T(\beta) = \int |1 + \beta z|^{2T} d\mu(z) = D_T^{(A)}(\beta) + D_T^{(A^c)}(\beta),$$

where the superscripts denote integration over  $A_\beta$  and  $A_\beta^c$  respectively. By boundedness of  $f$  and the previous estimates, we have

$$\frac{|N_T^{(A^c)}(\beta)|}{D_T^{(A)}(\beta)} \leq \|f\|_\infty \frac{(\phi(\beta) - \eta)^{2T}}{c(\phi(\beta) - \delta)^{2T}} \xrightarrow{T \rightarrow \infty} 0,$$

and

$$\frac{D_T^{(A^c)}(\beta)}{D_T^{(A)}(\beta)} \xrightarrow{T \rightarrow \infty} 0,$$

uniformly over  $\beta \in K$ . Hence,

$$\int f \, d\nu_{T,\beta} = \frac{N_T^{(A)}(\beta)}{D_T^{(A)}(\beta)} + o(1),$$

where  $o(1) \rightarrow 0$  uniformly in  $\beta \in K$ . Now, we restrict attention to the conditional probability measure on  $A_\beta$  with density proportional to  $|1 + \beta z|^{2T} \, d\mu(z)$ . On  $A_\beta$ , the function  $z \mapsto |1 + \beta z|$  attains its unique maximum at  $z^*(\beta)$ , since  $K \subset I \setminus \{-\alpha^*\}$  ensures that the active endpoint is unique, and the interval  $A_\beta$  can be made arbitrarily small by taking  $\varepsilon \downarrow 0$ . Since  $f$  is uniformly continuous on the compact set  $[\underline{Z}, \overline{Z}]$ , for any  $\varepsilon > 0$  we can shrink  $\varepsilon > 0$  (uniformly in  $\beta \in K$ ) so that

$$|f(z) - f(z^*(\beta))| < \varepsilon \quad \forall z \in A_\beta, \beta \in K.$$

Then,

$$\left| \frac{N_T^{(A)}(\beta)}{D_T^{(A)}(\beta)} - f(z^*(\beta)) \right| \leq \sup_{z \in A_\beta} |f(z) - f(z^*(\beta))| < \varepsilon,$$

because  $N_T^{(A)}(\beta)/D_T^{(A)}(\beta)$  is merely the expectation of  $f(Z)$  under the normalized weights  $|1 + \beta Z|^{2T} \mathbf{1}_{A_\beta} \, d\mu$ , where  $\mathbf{1}_{A_\beta}$  denotes the indicator of the set  $A_\beta$ . Combining this with the negligible contribution of  $A_\beta^c$ , we conclude that

$$\int f(z) \, d\nu_{T,\beta}(z) \longrightarrow f(z^*(\beta))$$

uniformly over  $\beta \in K$ . Since this holds for every bounded continuous  $f$ , we have  $\nu_{T,\beta} \rightarrow \delta_{z^*(\beta)}$ <sup>4</sup> weakly, uniformly over  $\beta \in K$ .  $\square$

The above result will be utilized in proving the following lemma establishing the uniform convergence of the derivatives of  $G_T$  over a compact interval omitting the point  $-\alpha^*$ . This will then yield a contradiction as the limiting derivative is strictly nonzero away from  $-\alpha^*$ . As a quick reminder from Appendix D, we defined

$$\alpha^* = \frac{2}{\underline{Z} + \overline{Z}}.$$

**Lemma E.8** (Asymptotics of the derivative). *Suppose Assumption 6.1 holds and the conditions of Remark E.4 are satisfied. Fix a compact interval  $K \subset I \setminus \{-\alpha^*\}$ , where  $I := (-2/\overline{Z}, 0)$ . Then:*

1. *The derivatives  $G'_T(\beta)$  converge uniformly on  $K$  to the derivative of  $\log \phi(\beta)$ :*

$$G'_T(\beta) \longrightarrow \frac{d}{d\beta} \log \phi(\beta)$$

*uniformly for  $\beta \in K$  as  $T \rightarrow \infty$ .*

2. *In particular, since  $-\alpha^* \notin K$ , there exist constants  $T_K < \infty$  and  $c_K > 0$  such that*

$$|G'_T(\beta)| \geq c_K > 0, \quad \forall \beta \in K, T \geq T_K.$$

*Proof.* We begin by writing

$$F_T(\beta) = \mathbb{E}[W] \frac{V_T(\beta)}{D_T(\beta)}, \quad V_T(\beta) := \text{Var}_\mu(u_T(\beta, Z)), \quad D_T(\beta) := \mathbb{E}_\mu[(1 - u_T(\beta, Z))^2].$$

Thus,

$$G_T(\beta) = \frac{1}{2T} (\log V_T(\beta) - \log D_T(\beta))$$

---

<sup>4</sup>By standard convention,  $\delta$  denotes a point-mass (Dirac measure).

and so

$$G'_T(\beta) = \frac{1}{2T} \frac{V'_T(\beta)}{V_T(\beta)} - \frac{1}{2T} \frac{D'_T(\beta)}{D_T(\beta)}. \quad (\text{E.12})$$

We analyze the two terms in (E.12) separately starting with the denominator term. For  $\beta \in K$  and  $z \in [\underline{Z}, \overline{Z}]$ , we have  $|1 + \beta z| \leq \phi_K < 1$ , thus

$$|u_T(\beta, z)| = |1 + \beta z|^T \leq \phi_K^T.$$

From the proof of Lemma E.7 we know that  $D_T(\beta) \rightarrow 1$  as  $T \rightarrow \infty$  uniformly in  $\beta \in K$ . Differentiating under the integral sign, we have

$$D'_T(\beta) = \mathbb{E}_\mu [2(1 - u_T)(-u'_T)],$$

where

$$u'_T(\beta, z) := \frac{d}{d\beta} u_T(\beta, z) = Tz(1 + \beta z)^{T-1}.$$

Therefore,

$$|D'_T(\beta)| \leq 2\mathbb{E}_\mu (|1 - u_T||u'_T|) \leq 4T\overline{Z}\phi_K^{T-1}$$

since  $|1 - u_T| \leq 1 + |u_T| \leq 2$  for large  $T$ . Consequently, for some constant  $C > 0$ ,

$$\left| \frac{1}{2T} \frac{D'_T(\beta)}{D_T(\beta)} \right| \leq C\phi_K^{T-1} \xrightarrow{T \rightarrow \infty} 0,$$

uniformly in  $\beta \in K$ , which shows that the second term in (E.12) is  $o(1)$  uniformly on  $K$ . The prior differentiation under the integral sign was justified by dominated convergence:  $|(1 - u_T)(-u'_T)| \leq 2T\overline{Z}\phi_K^{T-1}$  which is integrable w.r.t.  $\mu$  and independent of  $z$ , and for each fixed  $z$  the integrand is  $C^1$  in  $\beta$ .

We now turn to the numerator term of (E.12):  $\frac{1}{2T} \frac{V'_T(\beta)}{V_T(\beta)}$ . Since  $V_T(\beta) = \mathbb{E}_\mu[u_T^2] - \mathbb{E}_\mu[u_T]^2$  with  $u_T := u_T(\beta, Z)$ , differentiating, we obtain

$$V'_T(\beta) = \frac{d}{d\beta} \mathbb{E}_\mu[u_T^2] - 2\mathbb{E}_\mu[u_T] \frac{d}{d\beta} \mathbb{E}_\mu[u_T].$$

As above,

$$\left| \frac{d}{d\beta} \mathbb{E}_\mu[u_T] \right| \leq T\overline{Z}\phi_K^{T-1}, \quad \left| \frac{d}{d\beta} \mathbb{E}_\mu[u_T^2] \right| \leq 2T\overline{Z}\phi_K^{2T-1},$$

uniformly over  $\beta \in K$ . By (E.4) and (E.10) from Lemma E.7, we have  $V_T(\beta) \asymp \phi(\beta)^{2T}$  uniformly on  $K$ ; in particular, there exist constants  $0 < c_1 \leq c_2 < \infty$  such that

$$c_1\phi(\beta)^{2T} \leq V_T(\beta) \leq c_2\phi(\beta)^{2T} \quad \forall \beta \in K$$

for all  $T$  sufficiently large. Hence, the contribution from the term  $-2\mathbb{E}_\mu[u_T] \frac{d}{d\beta} \mathbb{E}_\mu[u_T]$  to the ratio  $\frac{1}{2T} \frac{V'_T(\beta)}{V_T(\beta)}$  can be bounded as

$$\left| \frac{1}{2T} \frac{-2\mathbb{E}_\mu[u_T] \frac{d}{d\beta} \mathbb{E}_\mu[u_T]}{V_T(\beta)} \right| \leq C'\phi_K^{T-1} \xrightarrow{T \rightarrow \infty} 0,$$

uniformly over  $\beta \in K$ , for some constant  $C' > 0$ . Thus, the main contribution to  $\frac{1}{2T} \frac{V'_T(\beta)}{V_T(\beta)}$  comes from  $\mathbb{E}_\mu[u_T^2]$ :

$$\frac{1}{2T} \frac{V'_T(\beta)}{V_T(\beta)} = \frac{1}{2T} \frac{\frac{d}{d\beta} \mathbb{E}_\mu[u_T(\beta, Z)^2]}{\mathbb{E}_\mu[u_T(\beta, Z)^2]} + o(1), \quad (\text{E.13})$$

uniformly over  $\beta \in K$ . Now

$$\mathbb{E}_\mu[u_T(\beta, Z)^2] = \int (1 + \beta z)^{2T} d\mu(z) \implies \frac{d}{d\beta} \mathbb{E}_\mu[u_T(\beta, Z)^2] = \int 2Tz(1 + \beta z)^{2T-1} d\mu(z).$$

and therefore

$$\frac{1}{2T} \frac{\frac{d}{d\beta} \mathbb{E}_\mu[u_T(\beta, Z)^2]}{\mathbb{E}_\mu[u_T(\beta, Z)^2]} = \frac{\int z(1 + \beta z)^{2T-1} d\mu(z)}{\int (1 + \beta z)^{2T} d\mu(z)} = \int \frac{z}{1 + \beta z} d\nu_{T,\beta}(z)$$

where  $\nu_{T,\beta}$  is precisely the probability measure from Lemma E.7(2). Combining with (E.13) and the negligibility of the denominator term, we obtain

$$G'_T(\beta) = \int \frac{z}{1 + \beta z} d\nu_{T,\beta}(z) + o(1), \quad (\text{E.14})$$

where  $o(1) \rightarrow 0$  uniformly over  $\beta \in K$ .

By Lemma E.7(2), for each fixed  $\beta \in K$  the measures  $\nu_{T,\beta}$  converge weakly to  $\delta_{z^*(\beta)}$ , where  $z^*(\beta) \in \{\underline{Z}, \overline{Z}\}$  is the endpoint at which  $\phi(\beta)$  is attained and this convergence is uniform in  $\beta \in K$ . Since the function  $(\beta, z) \mapsto \frac{z}{1 + \beta z}$  is continuous on  $K \times [\underline{Z}, \overline{Z}]$ , by uniform weak convergence,

$$\int \frac{z}{1 + \beta z} d\nu_{T,\beta}(z) \longrightarrow \frac{z^*(\beta)}{1 + \beta z^*(\beta)},$$

uniformly over  $\beta \in K$ . Together with (E.14), this yields

$$G'_T(\beta) \longrightarrow \frac{z^*(\beta)}{1 + \beta z^*(\beta)}$$

uniformly over  $\beta \in K$ . Now, on any compact  $K \subset I$  that does not contain  $-\alpha^*$ , the active endpoint  $z^*(\beta)$  is constant (always  $\underline{Z}$  or always  $\overline{Z}$ ), and the sign of  $1 + \beta z^*(\beta)$  is fixed. Therefore,

$$\frac{d}{d\beta} \log \phi(\beta) = \frac{d}{d\beta} \log |1 + \beta z^*(\beta)| = \frac{z^*(\beta)}{1 + \beta z^*(\beta)}.$$

and so  $G'_T(\beta) \longrightarrow \frac{d}{d\beta} \log \phi(\beta)$  as  $T \rightarrow \infty$  uniformly over  $\beta \in K$ , which proves part (1).

We can now wrap up the proof by establishing the second statement of the lemma. Note that the function  $\phi$  is smooth on  $I \setminus \{-\alpha^*\}$  and  $-\alpha^*$  is the unique minimizer of  $\phi$ . Hence  $\frac{d}{d\beta} \log \phi(\beta)$  is continuous and nonzero on  $K$ , and therefore there exists  $c_K > 0$  such that

$$\left| \frac{d}{d\beta} \log \phi(\beta) \right| \geq 2c_K$$

for all  $\beta \in K$ . By uniform convergence of  $G'_T$  to  $\frac{d}{d\beta} \log \phi(\beta)$  on  $K$ , we may choose  $T_K$  large enough so that

$$|G'_T(\beta)| \geq c_K$$

for all  $\beta \in K$  when  $T \geq T_K$ . This proves part (2) and completes the proof.  $\square$

The full result of Theorem 6.3 will now follow by a simple proof by contradiction by extracting a subsequence  $(\beta_{T_k}^*)_{k \geq 1}$  converging in the interior of the interval. The culmination of this section is now provided in the next result.

**Theorem E.9.** *Suppose the assumptions of Theorem E.6 hold. Let  $(\alpha_T^*, \beta_T^*)$  denote the limit of gradient flow on the two-parameter,  $T$ -layer, CA model whose existence is guaranteed by Theorem E.6. Moreover, assume that  $\lim_{T \rightarrow \infty} \beta_T^* \notin \{-2/\overline{Z}, 0\}$ . Then,*

$$\lim_{T \rightarrow \infty} \alpha_T^* = \alpha^* = \frac{2}{\underline{Z} + \overline{Z}}.$$

and

$$\lim_{T \rightarrow \infty} \beta_T^* = -\alpha^*.$$

Hence, the model is Bayes optimal by Lemmas C.1 and C.2.

*Proof.* We assume for contradiction that  $\lim_{T \rightarrow \infty} \beta_T^* \neq -\alpha^*$ . Then, as  $(\beta_T^*)_{T \geq 1}$  is contained in the compact interval  $[-2/\bar{Z}, 0]$  with  $\lim_{T \rightarrow \infty} \beta_T^* \notin \{-2/\bar{Z}, -\alpha^*, 0\}$ , we extract a convergent subsequence  $(\beta_{T_k}^*)_{k \geq 1}$  with limit

$$\bar{\beta} := \lim_{k \rightarrow \infty} \beta_{T_k}^* \in (-2/\bar{Z}, 0) \setminus \{-\alpha^*\}.$$

Choose a compact interval

$$K \subset (-2/\bar{Z}, 0) \setminus \{-\alpha^*\}$$

such that  $\bar{\beta} \in \text{int}(K)$ . Then  $\beta_{T_k}^* \in K$  for all sufficiently large  $k$ . By Lemma E.8, it follows that  $|G'_{T_k}(\beta_{T_k}^*)| \geq c_K > 0$  for all sufficiently large  $k$ . This immediately contradicts the nature of  $(\beta_{T_k}^*)_{k \geq 1}$  as a sequence of stationary points for  $(G_{T_k})_{k \geq 1}$ . Therefore, one must have  $\bar{\beta} = -\alpha^*$  and as the subsequence  $(T_k)_{k \geq 1} \subseteq \mathbb{N}$  was arbitrary, convergence for the entire sequence  $(\beta_T^*)_{T \geq 1}$  to  $-\alpha^*$  holds:

$$\lim_{T \rightarrow \infty} \beta_T^* = -\alpha^*. \quad (\text{E.15})$$

Convergence of  $\lim_{T \rightarrow \infty} \alpha_T^* = \alpha^*$  follows from (E.15) and the identity  $\alpha_T^* = \alpha^*(\beta_T^*)$  for all  $T \geq 1$ .  $\square$

The above result concludes the proof of Theorem 6.3.

## F Visualization of the loss landscape

The rationale behind the initializations given in Theorem 6.3 and discussed in Section 6 is supported in Figure 4 which illustrates a steep valley along the curve  $\{(\alpha^*(\beta), \beta) : \beta \in (-2/(\bar{m} + 1), 0)\}$  as  $\alpha^*(\beta) \approx -\beta$  ( $\alpha^*(\beta) \rightarrow -\beta$  as  $T \rightarrow \infty$ ) in this window. To contrast our setting with a more sophisticated model, we also plot the loss landscape of the two-parameter model where pre-Layer Normalization [Xiong et al., 2020] is added between the LCA layers. Interestingly, this model reveals a similarly located and sized ravine in the loss landscape, hinting at the insights from our ablated setting to more complex models.

## G Ablation experiments on synthetic data

In this appendix, we examine the significance of the  $S_t$  skip-connection and the CA between the layer outputs  $(F_t)_{t \geq 0}$  and the original raw data  $X$ —displayed in Figure 1—on the data generating distribution compatible with Section 3 and Assumption 6.1. To this end, we compare, empirically, the trained performance of the one- and two-parameter LCA models defined in Section 5 against ablated models. We introduce three new architectures in the one- and two-parameter settings. First, consider the one-parameter LCA model without  $S_t$  (equivalently with  $\alpha \equiv 0$ )—that is, we modify (5.2) to be

$$\mathbf{F}_t = \mathbf{F}_{t-1} + \mathbf{A}_{t-1}$$

and operate with one learnable parameter as in Section 5. Second, building on the preceding model, we now set  $\mathbf{A}_t = \mathbf{A}(\mathbf{Q}_t, \mathbf{K}_t, \mathbf{V}_t)$  with

$$\mathbf{V}_t = \alpha \mathbf{F}_t, \quad \mathbf{K}_t = \mathbf{Q}_t = \mathbf{F}_t, \quad (\text{G.1})$$

so that  $\mathbf{A}_t$  is no longer a LCA implementation, but rather is LSA applied to  $\mathbf{F}_t$  with a single learnable parameter. We refer to this architecture as a “one-parameter deep LSA without  $S_t$ ” to delineate it from the single-layer LSA model of Section 4. Lastly, as a final trainable comparison, we consider the LSA modification given in (G.1) and re-introduce  $S_t$  (again producing two learnable parameters) in the architecture, and refer

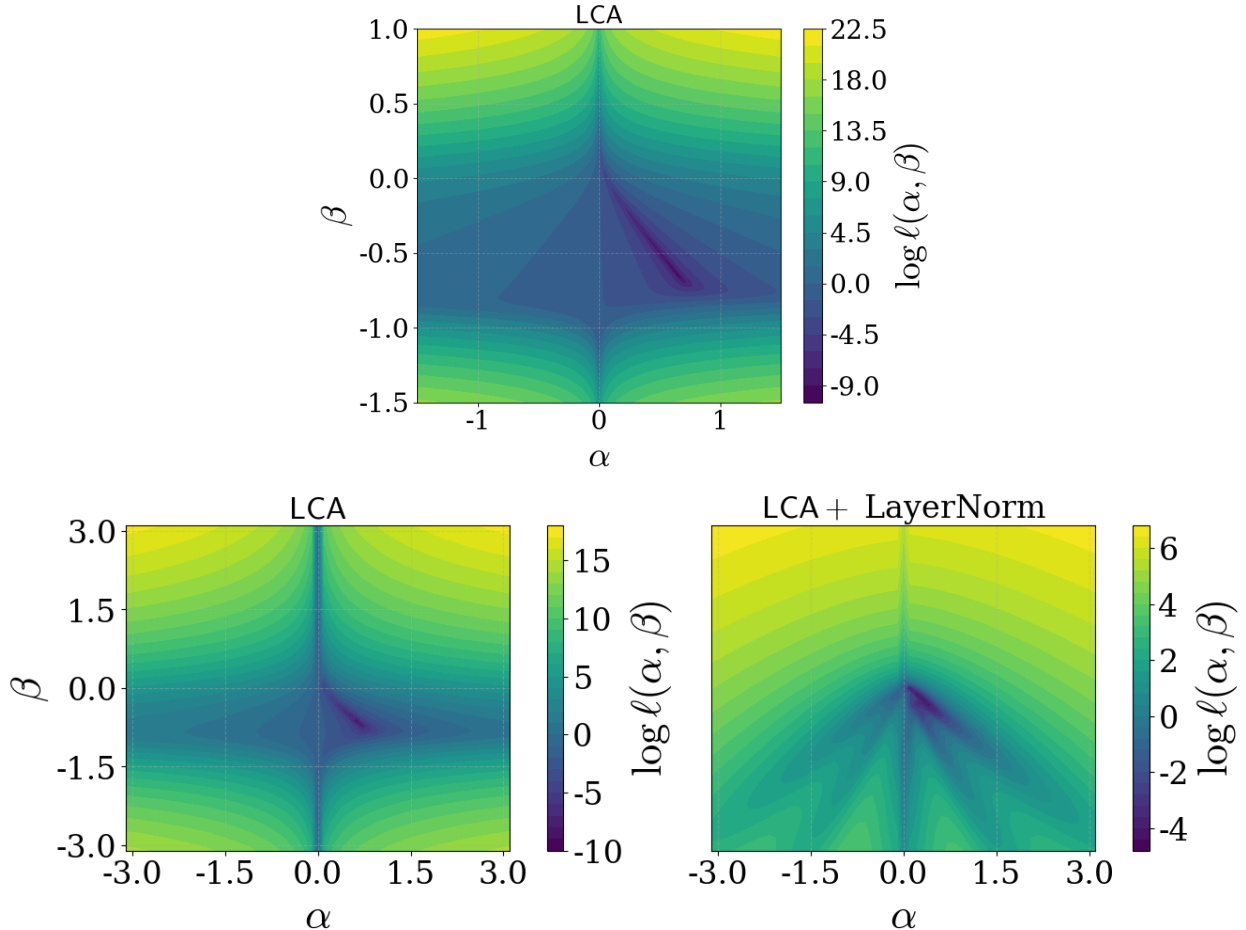


Figure 4: Log-scale heat map plots of the two-parameter loss  $\ell(\alpha, \beta)$  at depth  $T = 10$  (**top**) and  $T = 5$  (**bottom**) where  $\|\mathbf{m}\| \sim \text{Unif}(0, 2)$ . At depth  $T = 5$ , we compare the LCA-based model considered herein (**bottom left**) with the addition of pre-LayerNorm between the CA layers (**bottom right**).

to this ablation as a “two-parameter deep LSA.” As a naive baseline, we also consider the in-context sample mean:

$$\bar{y}_{L_{te}} = \frac{1}{L_{te}} \sum_{i=1}^{L_{te}} y_i.$$

In Figure 5, we see that the removal of the  $S_t$  skip-connection in the embedding architecture compromises model performance. Notably, in the simplified one-parameter setting, the ablated models fail to improve upon the naive in-context sample mean. Moreover, in Figure 6, we see that, swapping the LCA mechanism for LSA on  $F_t$  while keeping the  $S_t$  skip-connection deteriorates model performance, albeit improving upon the sample mean baseline and the single-layer LSA model. This further emphasizes the utility of the cross-attention and particularly of our novel  $S_t$  component.

## H Figures 2 and 3 experiment details

All models are trained using standard gradient descent (in place of gradient flow) on the non-asymptotic objective  $\ell_{N, L_{tr}}$  with  $N = 2000$  and  $L_{tr} = 100$ . Data is generated according to Section 3 with  $\zeta \sim \mathcal{N}(0, 1)$ ,

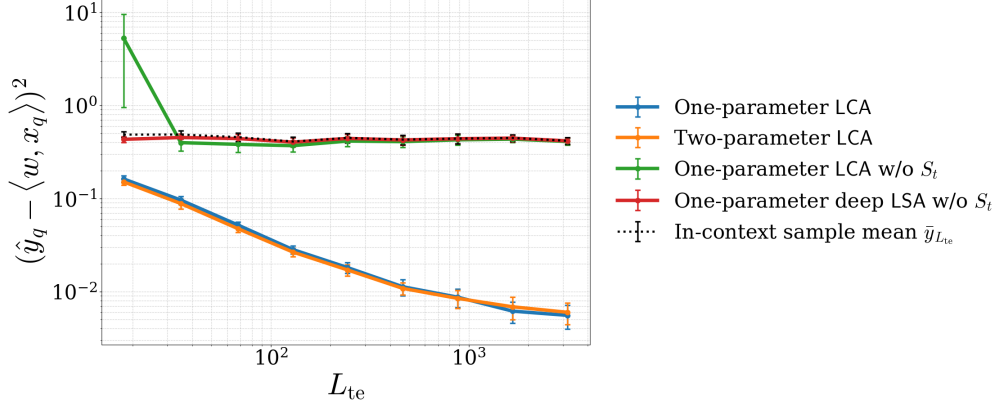


Figure 5: In-context performance at various  $L_{te}$  of one- and two-parameter LCA-based models, ablations without  $S_t$  ( $T = 10$ ), and the sample mean  $\bar{y}_{L_{te}}$ . Models are optimized on  $\ell_{N, L_{tr}}$  ( $L_{tr} = 100, N = 2000$ ) using gradient descent. Performance is averaged over 1000 test-prompts where error bars represent standard deviation over 10 separate training runs.

$d_1 = d_2 = 16$ , and  $\mathbf{m}$  drawn from a spherical Gaussian with norm mapped uniformly on  $[0, 5]$ .

**Further details for less-restricted LCA parametrizations (Figure 3).** We use the synthetic data-generating model discussed above. Throughout these experiments, we keep  $\mathbf{W}_t^K = \mathbf{W}_t^Q = \mathbf{I}_d$  fixed and train only the layerwise injection and value matrices  $(\mathbf{W}_t^S, \mathbf{W}_t^V)_{t=0}^{T-1}$ . We consider three increasingly flexible parametrizations where in all cases the weights are untied across layers unlike in the one- and two-parameter simplifications on which we base our theoretical results in Section 6. In the untied scalar model,

$$\mathbf{W}_t^S = \alpha_t \mathbf{I}_d, \quad \mathbf{W}_t^V = \beta_t \mathbf{I}_d,$$

where each layer has its own learnable pair  $(\alpha_t, \beta_t)$ . In the diagonal model,

$$\mathbf{W}_t^S = \text{diag}(\mathbf{b}_t), \quad \mathbf{W}_t^V = \text{diag}(\mathbf{b}_t),$$

where  $\mathbf{b}_t, \mathbf{b}_t \in \mathbb{R}^d$ . In the full-matrix model,  $\mathbf{W}_t^S, \mathbf{W}_t^V \in \mathbb{R}^{d \times d}$  are unconstrained trainable matrices.

All three models are initialized near the theory-predicted limiting parameters  $(\alpha^*, -\alpha^*)$  from Theorems 6.2–6.3. Specifically, with initial noise variance  $\sigma_{\text{init}} = 0.1$ , for the untied scalar model we initialize

$$\alpha_t = \alpha^* + \sigma_{\text{init}} g_t^S, \quad \beta_t = -\alpha^* + \sigma_{\text{init}} g_t^V,$$

with independent standard Gaussian variables  $g_t^S, g_t^V$ . For the diagonal model, we initialize

$$\mathbf{b}_t = \alpha^* \mathbf{1}_d + \sigma_{\text{init}} \mathbf{g}_t^S, \quad \mathbf{b}_t = -\alpha^* \mathbf{1}_d + \sigma_{\text{init}} \mathbf{g}_t^V,$$

where  $\mathbf{g}_t^S$  and  $\mathbf{g}_t^V$  have i.i.d. standard Gaussian entries and  $\mathbf{1}_d = [1 \cdots 1]^\top \in \mathbb{R}^d$ . For the full-matrix model, we initialize

$$\mathbf{W}_t^S = \alpha^* \mathbf{I}_d + \sigma_{\text{init}} \mathbf{G}_t^S, \quad \mathbf{W}_t^V = -\alpha^* \mathbf{I}_d + \sigma_{\text{init}} \mathbf{G}_t^V,$$

where the entries of  $\mathbf{G}_t^S, \mathbf{G}_t^V$  are i.i.d. standard Gaussian. Thus, each model has initialization biased near the theoretically optimal tied-scalar solution obtained in the one- and two-parameter models. However, the noise level  $\sigma_{\text{init}}$  is large with respect to the magnitude  $|\alpha^*|$  as the distribution on  $\mathbf{m}$  yields  $\alpha^* = 1/26 \approx 0.04$ .

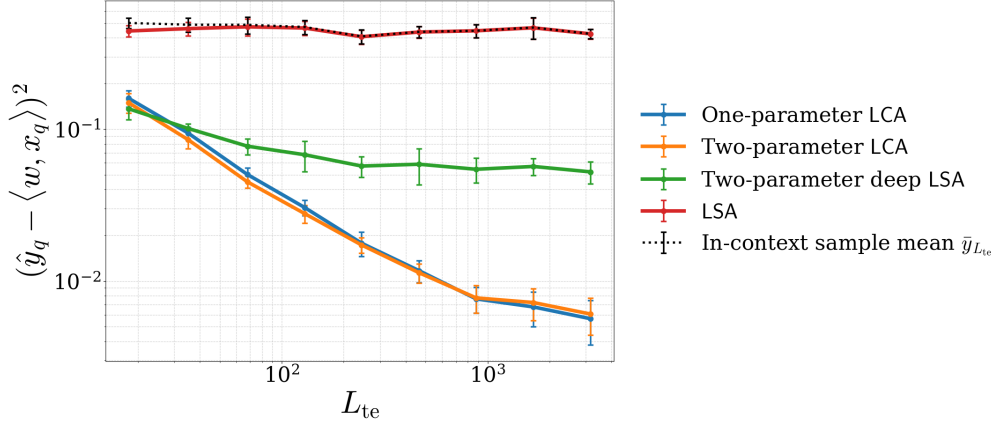


Figure 6: In-context performance at various  $L_{te}$  of one- and two-parameter LCA-based models, two-parameter deep LSA model ( $T = 10$ ), the LSA model from (4.2), and the sample mean  $\bar{y}_{L_{te}}$ . Models are optimized on  $\ell_{N, L_{tr}}$  ( $L_{tr} = 100, N = 2000$ ) using gradient descent. Performance is averaged over 1000 test-prompts where error bars represent standard deviation over 10 separate training runs.

Similarly to the protocol for Figure 2, we train each model by gradient descent on the empirical loss  $\ell_{N, L_{tr}}$  with  $N = 2000$  training prompts and training context length  $L_{tr} = 100$ . After training, in Figure 3, we display the scalar projections

$$\hat{\alpha}_t = d^{-1} \text{tr}(\mathbf{W}_t^S), \quad \hat{\beta}_t = d^{-1} \text{tr}(\mathbf{W}_t^V),$$

as well as the whitening diagnostic  $\|\mathbf{X}\mathbf{F}_t^\top/L - \mathbf{I}\|_F/\sqrt{d}$  following the heuristic laid out at the end of Section 6. The points/curves in Figure 3 are averaged over ten independent runs.

## I Table 1 experiment details

This appendix gives the implementation details for the corrupted avMNIST experiments in Table 1. The goal is to test whether the two architectural mechanisms isolated by the theory—cross-attention from an evolving state back to a fixed covariate sequence, and repeated re-injection of that fixed sequence—remain useful after replacing the linearized model (5.4) by conventional deep-learning components: convolutional token encoders, softmax multi-head attention, pre-layer normalization, MLP blocks, dropout, and a classification head.

Throughout this appendix, we use the same notation as Section 5 whenever possible. In particular,  $\mathbf{X}$  denotes the fixed encoded multimodal token sequence for one example,  $\mathbf{F}_t$  denotes the evolving state after  $t$  layers,  $\mathbf{A}_t$  denotes the attention update, and  $\mathbf{S}_t$  denotes the re-injection term. The only notational difference is that tokens are written as rows. Thus, in this appendix  $\mathbf{X}, \mathbf{F}_t \in \mathbb{R}^{L \times d}$ , whereas the theoretical sections write tokens as columns.

### I.1 Dataset, normalization, and task

We use a paired audio-visual MNIST dataset [Vielzeuf et al., 2019]. Each example is a triple

$$(I_i, A_i, c_i), \quad I_i \in \mathbb{R}^{1 \times 28 \times 28}, \quad A_i \in \mathbb{R}^{1 \times 28 \times 28}, \quad c_i \in \{0, 1, \dots, 9\},$$

where  $I_i$  is an image,  $A_i$  is a paired audio spectrogram, and  $c_i$  is the digit class. The experiments use the standard split stored in the repository: 60,000 training examples and 10,000 test examples. The image and audio arrays have spatial resolution  $28 \times 28$ ; a singleton channel dimension is added before passing them to the convolutional encoders. The data  $(I_i, A_i)$  is corrupted entry-wise by Gaussian noise to enforce difficulty in the learning task. Thereafter, the data is normalized to  $[0, 1]$ .

Each model outputs logits  $z_i \in \mathbb{R}^{10}$  and is trained with the cross-entropy loss

$$\ell_{\text{CE}}(z_i, c_i) = -\log \left( \frac{\exp(z_{i,c_i})}{\sum_{k=0}^9 \exp(z_{i,k})} \right).$$

## I.2 Common convolutional tokenization

For token dimension  $d$ , each modality encoder maps a  $28 \times 28$  input to 16 tokens in  $\mathbb{R}^d$ :

$$\Phi_I : \mathbb{R}^{1 \times 28 \times 28} \rightarrow \mathbb{R}^{16 \times d}, \quad \Phi_A : \mathbb{R}^{1 \times 28 \times 28} \rightarrow \mathbb{R}^{16 \times d}.$$

The two encoders have the same architecture but do not share weights. Each encoder consists of two convolution–ReLU layers, a  $2 \times 2$  max-pooling layer, two additional convolution–ReLU layers, a second  $2 \times 2$  max-pooling layer, adaptive average pooling to a  $4 \times 4$  grid, flattening into 16 tokens, and a final layer normalization. The hidden convolutional width is taken to be 16.

We add learned positional embeddings and learned modality embeddings:

$$\mathbf{X}_I^{(0)} = \Phi_I(I) + \mathbf{P}_I + \mathbf{M}_I, \quad \mathbf{X}_A^{(0)} = \Phi_A(A) + \mathbf{P}_A + \mathbf{M}_A,$$

where  $\mathbf{P}_I, \mathbf{P}_A \in \mathbb{R}^{16 \times d}$  are learned positional embeddings and  $\mathbf{M}_I, \mathbf{M}_A \in \mathbb{R}^{1 \times d}$  are learned modality embeddings broadcast over tokens. The fixed multimodal sequence is

$$\mathbf{X} = \text{concat}(\mathbf{c}, \mathbf{X}_I^{(0)}, \mathbf{X}_A^{(0)}) \in \mathbb{R}^{L \times d},$$

where  $\mathbf{c} \in \mathbb{R}^d$  is a learned CLS token.

## I.3 Paper-inspired multimodal architecture

The four paper-inspired models are empirical analogues of the CA recurrence (5.2). They keep a fixed encoded sequence  $\mathbf{X}$  and update an evolving state

$$\mathbf{F}_t \in \mathbb{R}^{L \times d}, \quad t = 0, 1, \dots, T.$$

The state is initialized from the fixed sequence by a learned affine map

$$\mathbf{F}_0 = \mathbf{X} \mathbf{W}_0^\top + \mathbf{1} b_0^\top.$$

This differs from the simplified theoretical initialization  $\mathbf{F}_0 = 0$ .

Each fusion layer has three possible components: an attention update, an optional re-injection of  $\mathbf{X}$ , and a feed-forward residual block. We use pre-layer normalization  $\text{LN}(\cdot)$  throughout. In the full model, the attention update is

$$\mathbf{A}_{t-1} = \text{MHA}_t(\text{LN}(\mathbf{F}_{t-1}), \text{LN}(\mathbf{X}), \text{LN}(\mathbf{X})),$$

Thus, as in (5.3), the evolving state attends back to the fixed encoded covariates.

The empirical re-injection term is a gated version of the theoretical term  $\mathbf{S}_{t-1} = \mathbf{W}_{t-1}^S \mathbf{X}$  which is used to provide stability during training. After the attention residual,

$$\tilde{\mathbf{F}}_t = \mathbf{F}_{t-1} + \mathbf{A}_{t-1},$$

we set

$$\mathbf{S}_{t-1} = \mathbf{G}_{t-1}(\tilde{\mathbf{F}}_t) \odot \left( \mathbf{X}(\mathbf{W}_{t-1}^S)^\top + \mathbf{1}(b_{t-1}^S)^\top \right),$$

where  $\odot$  denotes entrywise multiplication and

$$\mathbf{G}_{t-1}(\tilde{\mathbf{F}}_t) = \sigma \left( \tilde{\mathbf{F}}_t(\mathbf{W}_{t-1}^G)^\top + \mathbf{1}(b_{t-1}^G)^\top \right)$$

is a learned sigmoid gate. The full update is therefore

$$\bar{\mathbf{F}}_t = \tilde{\mathbf{F}}_t + \mathbf{S}_{t-1}, \quad \mathbf{F}_t = \bar{\mathbf{F}}_t + \text{FFN}_t(\text{LN}(\bar{\mathbf{F}}_t)),$$

where  $\text{FFN}_t$  is a two-layer pointwise MLP with GELU activation, dropout, and hidden width  $d_h$ .

The classifier uses the final CLS representation:

$$h = \mathbf{F}_T[\text{CLS}],$$

and maps  $h$  to logits in  $\mathbb{R}^{10}$  using layer normalization followed by a two-layer MLP head with GELU activation and dropout.

**Ablation axes.** The four paper-inspired models differ only in whether the attention update uses  $\mathbf{F}_t - \mathbf{X}$  cross-attention and whether the re-injection term  $\mathbf{S}_t$  is present:

- **Full paper-inspired model (Inj. & cross-attn):** uses the cross-attention update above and includes  $\mathbf{S}_t$ .
- **No injection:** uses the same  $\mathbf{F}_t - \mathbf{X}$  cross-attention update but sets  $\mathbf{S}_t \equiv 0$ .
- **No cross-attn:** keeps the re-injection term  $\mathbf{S}_t$ , but replaces the cross-attention update by self-attention on the evolving state,

$$\mathbf{A}_{t-1} = \text{MHA}_t(\text{LN}(\mathbf{F}_{t-1}), \text{LN}(\mathbf{F}_{t-1}), \text{LN}(\mathbf{F}_{t-1})).$$

- **No inj. & no cross-attn:** uses the self-attention update above and sets  $\mathbf{S}_t \equiv 0$ .

These ablations isolate the two mechanisms appearing in (5.2)–(5.3): access to the fixed sequence  $\mathbf{X}$  through cross-attention, and layer-wise re-injection of  $\mathbf{X}$  through  $\mathbf{S}_t$ .

## I.4 Bidirectional cross-attention baseline

The standard bidirectional baseline does not maintain a single evolving state  $\mathbf{F}_t$  and does not re-inject a fixed sequence. Instead, it maintains separate image and audio streams

$$\mathbf{U}_t, \mathbf{V}_t \in \mathbb{R}^{16 \times d}, \quad \mathbf{U}_0 = \Phi_I(I) + \mathbf{P}_I, \quad \mathbf{V}_0 = \Phi_A(A) + \mathbf{P}_A.$$

At layer  $t$ , the image stream attends to the audio stream and the audio stream attends to the image stream:

$$\tilde{\mathbf{U}}_t = \mathbf{U}_{t-1} + \text{MHA}_t^I(\text{LN}(\mathbf{U}_{t-1}), \text{LN}(\mathbf{V}_{t-1}), \text{LN}(\mathbf{V}_{t-1})),$$

$$\tilde{\mathbf{V}}_t = \mathbf{V}_{t-1} + \text{MHA}_t^A(\text{LN}(\mathbf{V}_{t-1}), \text{LN}(\mathbf{U}_{t-1}), \text{LN}(\mathbf{U}_{t-1})).$$

Each stream is then updated by its own feed-forward residual block:

$$\mathbf{U}_t = \tilde{\mathbf{U}}_t + \text{FFN}_t^I(\text{LN}(\tilde{\mathbf{U}}_t)), \quad \mathbf{V}_t = \tilde{\mathbf{V}}_t + \text{FFN}_t^A(\text{LN}(\tilde{\mathbf{V}}_t)).$$

The final representation is obtained by mean-pooling each stream and concatenating the two pooled vectors:

$$h = \text{concat} \left( \frac{1}{16} \sum_{j=1}^{16} \mathbf{U}_T[j], \frac{1}{16} \sum_{j=1}^{16} \mathbf{V}_T[j] \right) \in \mathbb{R}^{2d}.$$

A layer-normalized two-layer MLP head maps  $h$  to logits in  $\mathbb{R}^{10}$ . This baseline lacks the two paper-specific components: a single evolving state repeatedly attending to a fixed  $\mathbf{X}$ , and recurrent re-injection of  $\mathbf{X}$ .

## I.5 Training and reporting

All models in Table 1 are trained under the same optimization budget. The hyperparameters are

$$d = 16, \quad T = 10, \quad \text{number of heads} = 4, \quad d_h = 32, \quad g = 4, \quad \text{dropout} = 0.1.$$

We train for 100 epochs using AdamW with standard specifications: learning rate  $3 \times 10^{-4}$  and weight decay  $10^{-4}$ . The batch size is 256. The best test accuracy of each model is reported. Obtaining the results displayed in Table 1 totaled approximately five hours of runtime on a single NVIDIA H200 GPU.